



**ATMOSPHERIC TEMPERATURE PROFILES
BY GROUND-BASED INFRARED
SPECTROMETER MEASUREMENTS**

THESIS

Jon M. Saul, First Lieutenant, USAF

AFIT/GM/ENP/00M-11

**DEPARTMENT OF THE AIR FORCE
AIR UNIVERSITY
AIR FORCE INSTITUTE OF TECHNOLOGY**

Wright-Patterson Air Force Base, Ohio

20001113 029

APPROVED FOR PUBLIC RELEASE; DISTRIBUTION UNLIMITED

DIGITAL QUALITY ASSURANCE 4

AFIT/GM/ENP/00M-11

ATMOSPHERIC TEMPERATURE PROFILES
BY GROUND-BASED INFRARED
SPECTROMETER MEASUREMENTS

THESIS

JON M. SAUL, FIRST LIEUTENANT, USAF

AFIT/GM/ENP/00M-11

Approved for public release; distribution unlimited

The views expressed in this thesis are those of the author and do not reflect the official policy or position of the United States Air Force, Department of Defense, or the U. S. Government.

ATMOSPHERIC TEMPERATURE PROFILES BY GROUND-BASED INFRARED
SPECTROMETER MEASUREMENTS

THESIS

Presented to the Faculty of the Graduate School of Engineering and Management
of the Air Force Institute of Technology
Air University
Air Education and Training Command
in Partial Fulfillment of the Requirements for the
Degree of Master of Science in Meteorology

Jon M. Saul, B.S.
First Lieutenant, USAF

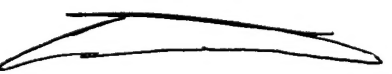
March 2000

Approved for public release; distribution unlimited

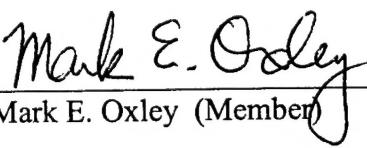
ATMOSPHERIC TEMPERATURE PROFILES BY GROUND-BASED INFRARED
SPECTROMETER MEASUREMENTS

Jon M. Saul, B.S.
First Lieutenant, USAF

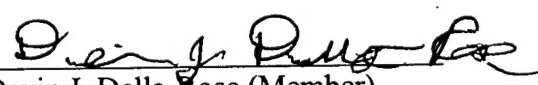
Approved:


Glen P. Perram (Chairman)

3 MAR 00
date


Mark E. Oxley (Member)

3 Mar 00
date


Devin J. Della-Rose (Member)

3 Mar 00
date

Acknowledgments

I wish to thank Lieutenant Colonel Glen Perram, my advisor, for providing me with the support and opportunity to conduct this research. His expertise and encouragement kept me on track and was always uplifting.

Also, I wish to thank Major Darrel Goldenstein for sparking my interest in the area of remote sensing and providing the background information need for this research.

Captain Roy Calfas, from the Air Force Research Laboratory (AFRL), is greatly appreciated for supplying the up-to-date versions of the PLEXUS atmospheric software and his ability to answer technical question about the software.

Jon M. Saul

Table of Contents

Acknowledgments	v
List of Figures	viii
List of Tables	x
Abstract	xi
ATMOSPHERIC TEMPERATURE PROFILES BY GROUND-BASED INFRARED SPECTROMETER MEASUREMENT	
I. Introduction	
1.1 Summary	1
1.2 Statement of Problem	2
1.3 Overview	3
II. Literature Review	
2.1 Atmospheric Radiation Theory	4
2.2 Retrieval Approaches	7
2.3 Atmospheric Model	
2.3.1 PLEXUS	9
2.3.2 SHARC and MODTRAN Merged (SAMM)	11
2.4 Bomem MR-154 Spectrometer	11
III. Methodology	
3.1 Overview	15
3.2 Spectral Region Determination	17
3.3 Calculating Kernel Functions	21
3.4 Calculating Atmospheric Brightness Temperature Functions	23
3.5 Collecting Atmospheric Radiance Measurements	25
3.5.1 Spectrometer Setup	25
3.5.2 Spectrometer Calibration	26
3.5.3 Acquiring Atmospheric Radiometric Data	26
3.6 Computing Atmospheric Temperature Profiles	27

IV.	Results	
4.1	Introduction	28
4.2	Spectral Range Determination	28
4.3	Collecting Atmospheric Radiance Measurements	29
4.4	Computing Atmospheric Temperature Profiles	
4.4.1	Test Case I: 1 December 1999	31
4.4.1	Test Case II: 8 December 1999	34
4.4.3	Summary	36
V.	Conclusions and Recommendations	37
Appendix 1: Brightness Temperature and Transmittance Function Data		39
Appendix 2: IDL Programs and Mathcad Templates		52
Appendix 3: Radiosonde Data		67
Bibliography		68
Vita		69

List of Figures

Figure	Page
2.1 Example of graphical radiance output from PLEXUS.	10
2.2 Example of graphical transmittance output from PLEXUS.	10
2.3 Bomem MR-154 Basic Components.	13
2.4 Principle of operation of the FTIR spectrometer.	14
3.1 PLEXUS graphical radiance output for 15 January 2000.	19
3.2 PLEXUS graphical radiance output for 15 July 1999.	19
3.3 Ratio of 15 July 1999 and 15 January 2000 radiances.	20
3.4 Ratio of 15 January 2000 and 15 July 1999 Transmissivity	20
3.5 Example of output from best-fit software using values from Table 3.3.	22
3.6 Temperature profile used by PLEXUS for 15 November 1999.	23
3.7 Best-fit brightness temperature function using Table 3.4 data.	25
4.1 Calibrated spectrometer output for 1 December 1999.	30
4.2 Calibrated spectrometer output for 8 December 1999.	30
4.3 Temperature plots for 1 December 1999.	32
4.4 Temperature plots for 1 December 1999.	32
4.5 Plot of ΔB using 1 December 1999 radiosonde data.	33
4.6 Plots of $\Delta B(z)$ for 1 December 1999.	33
4.7 Temperature plots for 8 December 1999.	34
4.8 Temperature plots for 8 December 1999.	35
4.9 Plot of ΔB using 8 December 1999 radiosonde data..	35

4.10 Plots of $\Delta B(z)$ for 8 December 1999.	36
A.1.1 Plot of brightness temperature data points and fitted function.	41
A.1.2 Residual Plot of fitted brightness temperature function.	41
A.1.3 Plot of transmittance values and fitted function for 2566 cm^{-1} .	43
A.1.4 Residual plot of fitted transmittance function for 2566 cm^{-1} .	43
A.1.5 Plot of transmittance values and fitted function for 2567 cm^{-1} .	45
A.1.6 Residual plot of fitted transmittance function for 2567 cm^{-1} .	45
A.1.7 Plot of transmittance values and fitted function for 2568 cm^{-1} .	47
A.1.8 Residual plot of fitted transmittance function for 2568 cm^{-1} .	47
A.1.9 Plot of transmittance values and fitted function for 2569 cm^{-1} .	49
A.1.10 Residual plot of fitted transmittance function for 2569 cm^{-1} .	49
A.1.11 Plot of transmittance values and fitted function for 2570 cm^{-1} .	51
A.1.12 Residual plot of fitted transmittance function for 2570 cm^{-1} .	51

List of Tables

Table	Page
3.1 Highly Variable Atmospheric Constituents and their Absorption Bands.	18
3.2 Pathlengths used in calculation of transmittance.	21
3.3 Examples of transmittance values for specific pathlengths.	22
3.4 Example of temperature and calculated brightness temperatures for 2568 cm^{-1} .	24
4.1 Most promising frequencies.	29
4.2 Atmospheric radiance measurements collected by the spectrometer.	31
A.1.1 Numeric Summary of fitted brightness temperature function parameters.	40
A.1.2 Numeric summary for transmittance and kernel parameters for 2566 cm^{-1} .	42
A.1.3 Numeric summary for transmittance and kernel parameters for 2567 cm^{-1} .	44
A.1.4 Numeric summary for transmittance and kernel parameters for 2568 cm^{-1} .	46
A.1.5 Numeric summary for transmittance and kernel parameters for 2569 cm^{-1} .	48
A.1.6 Numeric summary for transmittance and kernel parameters for 2570 cm^{-1} .	50

Abstract

A method to recover atmospheric temperature profiles using a ground-based Fourier Transform Infrared spectrometer was investigated. The method used a difference form of the radiative transfer equation, a Bomem MR series Fourier Transform Infrared Spectrometer to collect atmospheric radiance values, and the Phillips Laboratory Expert-assisted User Software (PLEXUS) atmospheric radiance model, to recover an atmospheric temperature profile. The method researched uses radiance values from both the spectrometer measurements and the atmospheric model, along with kernel functions calculated by the atmospheric model as input to a difference form of the radiation transfer equation. From this the change in brightness temperatures was determined. The method assumes that the actual brightness temperature profile is a summation of a standard or reference brightness temperature profile plus some change in the brightness temperature. The brightness temperature profile used by the atmospheric model is the reference brightness temperature profile. Planck's Law was employed to transform the calculated brightness temperature function into a temperature function. A temperature profile was retrieved, although significant differences existed between the recovered temperature profile and a radiosonde recovered temperature profile.

ATMOSPHERIC TEMPERATURE PROFILES BY GROUND-BASED INFRARED SPECTROMETER MEASUREMENT

I. Introduction

1.1 Summary

In the last decade, great strides have been made in the area of remote sensing by surface based equipment. Advances in technology and reduction in the cost associated in the manufacture of remote sensing equipment have made the plausibility of remote sensing a reality. In particular, remote sensors are sought for as a means of replacing or accenting current atmospheric measurement techniques.

Radiosondes are the principle devices used to obtain atmospheric profiles. A single radiosonde costs approximately \$100. Typically, radiosonde sites launch radiosondes twice a day. Even with these conservative costs, a yearly supply of radiosondes for one station can cost over \$73,000. This estimate does not include the cost of tracking the radiosonde or disseminating the data. Using surface-based remote sensors, atmospheric profiles can be recovered (Smith et al. 1990). The infrared spectrometer is one instrument being studied for its use in obtaining infrared spectral data to produce atmospheric profiles. Smith et al. (1990) believes a basic interferometer system capable of performing ground-based atmospheric profiling would cost less than \$50,000. A ground-based infrared spectrometer system offers the possibility of saving millions of dollars annually.

A problem with the current profiling system, radiosondes, is the temporal resolution of upper air profiles. Typically, radiosondes are launched twice a day, at 00Z and 12Z, and recover one atmospheric profile for each radiosonde launched. Because

atmospheric profiles of the troposphere are constantly changing, the recovery of atmospheric profiles twice a day leaves large temporal gaps in the data. An infrared spectrometer has the ability to produce atmospheric radiance measurements every few seconds. From these radiance measurements, a profile can be calculated for each radiance measurement. An increased temporal resolution provided by ground-based spectrometers will enhance all areas of meteorology.

With the cost and the temporal coverage benefits, the use of an infrared spectrometer to supplement or replace the radiosondes as the primary mean of retrieving atmospheric profiles looks promising. The remaining question is which process to use to recover atmospheric profiles.

1.2 Statement of Problem

This research used a difference form of the radiative transfer equation, a Bomem MR series Fourier Transform Infrared Spectrometer (FTIR) to collect atmospheric radiance values, and the Phillips Laboratory Expert-assisted User Software (PLEXUS) atmospheric radiance model, to recover an atmospheric temperature profile. The method researched uses radiance values from spectrometer measurements and the atmospheric model, along with transmissivity value calculated by the atmospheric model as input to the difference form of the radiation transfer equation. From this the change in brightness temperatures can be determined. The method assumes that the actual brightness temperature profile is a summation of a standard or reference brightness temperature profile plus some change in the brightness temperature. The brightness temperature profile used by the atmospheric model is the reference brightness temperature profile. The goal is to determine the changes in the atmospheric brightness temperature profile

and to recover the actual brightness temperature profile. The temperature profile can be calculated using the relationship between brightness temperature and temperature in Planck's Law.

1.3 Overview

This thesis consists of five chapters. Chapter II contains literature review material, which contains fundamental material to support this research. Chapter III describes the procedures used during this research. Chapter IV presents the results of this research. Chapter V discusses conclusions made from this research.

II. Literature Review

2.1 Atmospheric Radiation Theory

The concept of using radiative transfer to formulate the absorbing, scattering, and creation of natural radiation within a volume filled with particles interacting with radiation was developed for astrophysical problems (Schanda, 1986). Radiation can be absorbed by atmospheric gases in continuum: (ionization and photo-dissociation), and discrete (electronic transitions, vibrational transitions, and rotational transitions) bands. In the infrared region, vibrational and rotational transitions account for most of spectral line emissions (Goody and Young, 1989). Transitions between two energy levels produce discrete spectral line emission or absorption, but due to molecule collision, spectral broadening occurs and distorts a molecule's energy levels. This distortion in the energy level causes the transitions to occur over a range of frequencies instead of one discrete frequency.

The radiative transfer equation (RTE) accounts for all four possible radiative interactions: the emission of radiation by a gas, the absorption of radiation by a gas, the scattering of radiation out of a beam, and the scattering of radiation into a beam. A general formula for the instantaneous change of the radiance is:

$$\frac{\partial L}{\partial s} = A + B + C + D \quad (2.1)$$

where,

L = monochromatic radiance ($\text{W}/\text{cm}^2 \text{ cm}^{-1} \text{ sr}$)

s = distance along a beam (meters)

A = absorption of radiation by a gas ($\text{W}/\text{cm}^2 \text{ cm}^{-1} \text{ m}^{-1}$)

B = emission of radiation by a gas ($\text{W}/\text{cm}^2 \text{ cm}^{-1} \text{ m}^{-1}$)

C = scattering of radiation out of a beam ($\text{W}/\text{cm}^2 \text{ cm}^{-1} \text{ m}^{-1}$)

D = scattering of radiation into a beam ($\text{W}/\text{cm}^2 \text{ cm}^{-1} \text{ m}^{-1}$)

A special case of the RTE is sometimes referred to as the Schwarzschild's equation. The Schwarzschild equation assumes no scattering of radiation into or out of the beam. On a clear, cloudless day the Schwarzschild's equation (Wallace, 1997), Equation 2.2, is valid for the atmosphere, and is:

$$L_\lambda = L_{0_\lambda} + \int_0^\infty B_\lambda(z) W_\lambda(z, \mu) dz \quad (2.2)$$

where,

L_{0_λ} = spectral radiance at the top of the atmosphere ($\text{W}/\text{cm}^2 \text{ cm}^{-1} \text{ sr}$)

L_λ = spectral radiance received ($\text{W}/\text{cm}^2 \text{ cm}^{-1} \text{ sr}$)

$\mu = \cos(\theta)$

θ = zenith angle

$B_\lambda(z)$ = blackbody radiance ($\text{W}/\text{cm}^2 \text{ cm}^{-1}$)

$W_\lambda(z, \mu)$ = kernel function (change of transmittance with respect to height)

z = height (meters)

λ = wavelength (meters)

Retrieval approaches use an inverse form of the radiative transfer equation to solve for atmospheric temperature profiles. Using the Schwarzschild's form of the radiative transfer, Equation (2.2), and calibrated radiance values obtained from an infrared spectrometer, it is possible to calculate a temperature profile. This version of the

radiative transfer equation assumes no scattered or diffuse radiation. These assumptions are viable for the infrared spectrum in the atmosphere in the absence of clouds (Kidder and Vonder Haar, 1995).

A linear approximation for the radiative transfer equation in a matrix form is (Schanda, 1986):

$$\vec{L}_\lambda = W_\lambda \vec{B}_\lambda \quad (2.3)$$

where,

\vec{L}_λ = vector of monochromatic radiance values ($\text{W}/\text{cm}^2 \text{ cm}^{-1} \text{ sr}$)

W_λ = a matrix of change in transmittance values

\vec{B}_λ = vector of brightness temperatures ($\text{W}/\text{cm}^2 \text{ cm}^{-1}$)

Using the ground-based spectrometer, the measured radiance, L_λ , is observed and the weighting functions, $W_\lambda(z, \mu)$, can be calculated using an atmospheric model. An inverse method uses the observed radiances to calculate a Planck's radiance profile. The inverse of the non-scattering radiative transfer equation is:

$$W_\lambda^{-1} \vec{L}_\lambda = \vec{B}_\lambda \quad (2.4)$$

With B_λ known, then temperature is calculated using Planck's function.

$$B_\lambda = C_1 \lambda^{-5} / [\exp(C_2 / \lambda T) - 1]$$

(2.5)

where,

B_λ = brightness temperature ($\text{W}/\text{cm}^2 \text{ cm}^{-1}$)

T = temperature (Kelvin)

λ = wavelength (meters)

$$C_1 = 1.1919439 \times 10^{-16} \text{ W m}^2$$

$$C_2 = 1.438769 \times 10^{-2} \text{ m K}$$

2.2 Retrieval Approaches

In late 1988, researchers conducted the Ground-based Atmospheric Profiling Experiment (GAPEX) (Smith et al, 1990). One part of GAPEX involved using a high-resolution interferometer (HIS) to measure the infrared spectrum. Atmospheric temperature and water vapor profiles were calculated using the measured radiances from the HIS. Researchers used the inverse of the non-scattering radiative transfer matrix, Equation 2.4, to recover temperature profiles. The HIS was used to obtain atmospheric radiance data and statistical data was used to determine the kernel function.

In mid 1992, researchers experimented with retrieving atmospheric profiles from radiance values obtained by a Double Beam Interferometer Sounder (DBIS) (Therlault 1993); (Therlault et al, 1996). The DBIS experiment used the approach based on the minimum information method. There are two main advantages to this approach: one, "first-guess" profiles are not required, and second, simultaneous retrieval for multiple parameters is possible.

The method works as follows: first, researchers assumed that the measured radiance is a function of the actual radiance plus a linear perturbation (Therlault 1993); (Therlault et al, 1996). The perturbations are linearized about a point L_0 ,

$$L(v) = L_0(v) + dL(v) \quad (2.6)$$

where $L(v)$ is the measured spectral radiance, $L_0(v)$ is the actual radiance, and $dL(v)$ is the perturbation of the radiance. Second, the approach employs a linear difference technique in a matrix form.

$$B_\lambda = [W^T S_e^{-1} W + S_b^{-1}]^{-1} W^T S_e^{-1} L_\lambda \quad (2.7)$$

This approach constrains the solution by weighting the equation with two error matrices, S_e and S_b . The error weighting matrices accounts for instrument error and uncertainty in the "first-guess" profile.

Obtaining the damping matrix, S_b , poses a problem (Theriault 1993:); (Theriault et al, 1996). The selection of the damping matrix must be completed empirically. Another problem deals with the time required to iterate to a solution.

In another experiment, researchers at the University of Wisconsin-Madison use the Atmospheric Emitted Radiance Interferometer (AERI) to measure atmospheric radiance every ten minutes. Atmospheric temperature profiles were produced using the measured radiance. AERI uses an inverse technique to retrieve a temperature profile from ground-based radiance measurements. Using the inverse of the radiative transfer equation, researchers at the University of Wisconsin-Madison use a statistical first guess of an atmospheric temperature profile and the measured radiances to solve the inverse radiative transfer equation. The University of Wisconsin-Madison has detailed information on the AERI project at <http://cimss.ssec.wisc.edu/aerlwww/aeri/>.

Hauser (1999) experimented with the Bomem MR-154 FTIR spectrometer to recover infrared radiance measurements of the atmosphere. The retrieval method used a least squares solution to obtain a temperature profiles from observed radiances. The method

involves multiplying both sides of equation 2.2 by the transpose of the weighting function, which Hauser identifies as the “kernel”, and solving for blackbody temperatures. The weighting functions or kernels, W , are the changes in monochromatic transmissivity over path length. MODTRAN calculations are used to compute the weighting functions. Once the weighting function was determined, the inverse matrix was solved.

$$L_\lambda W_\lambda^{-1} = B_\lambda \quad (2.8)$$

In his results, Hauser (1999) states that the procedure did not work, but gives no explanation as to why.

2.3 Atmospheric Models

2.3.1 PLEXUS

PLEXUS is a user-oriented software platform, which integrates user input into DOD standard atmospheric and celestial models. PLEXUS provides a graphical interface for the following Air Force Research Lab (AFRL) codes: MODTRAN3.7, SAMM1, FASCODE3P, and SAG1. The PLEXUS software allows the user to input parameters, then the PLEXUS software converts the numeric input to the native units of the applicable AFRL code. The source codes of the models are not altered in any way. PLEXUS is available on a CD through AFRL (PLEXUS, 1999).

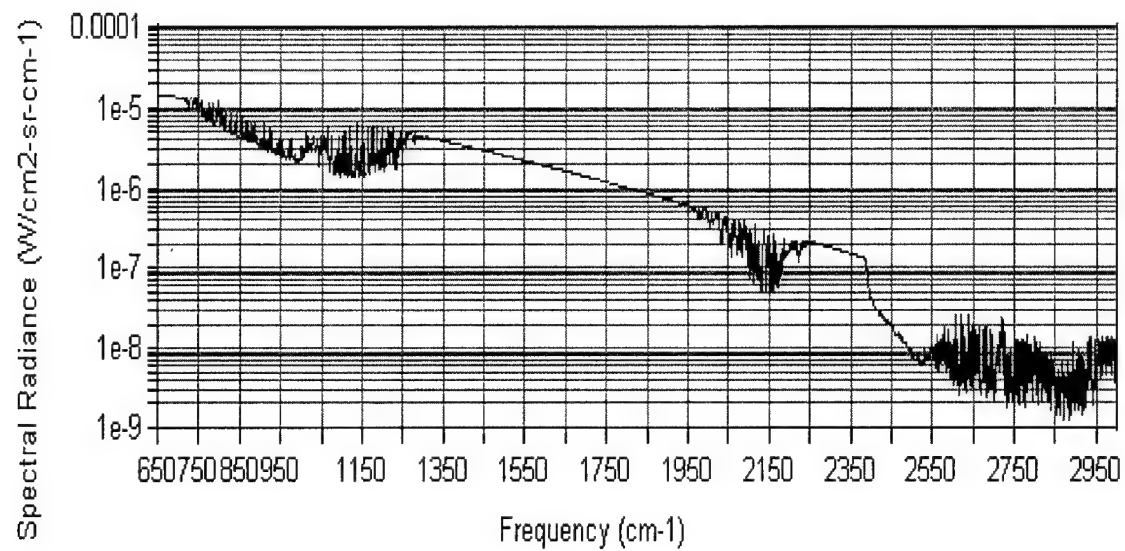


Figure 2.1 Example of graphical radiance output from PLEXUS.

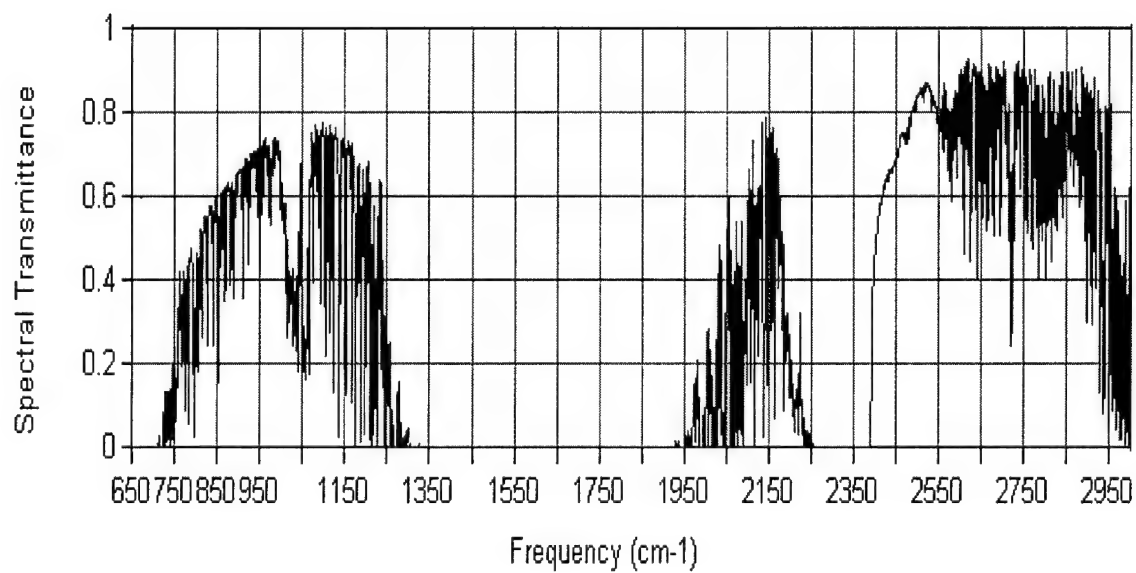


Figure 2.2 Example of graphical transmittance output from PLEXUS.

2.3.2 SHARC and MODTRAN Merged (SAMM)

The SAMM model was used to calculate all model derived transmittance and radiance data. SAMM is an atmospheric model, which combines the Moderate Resolution Transmittance Model (MODTRAN) and the Strategic High-Altitude Atmospheric Radiance Code (SHARC). MODTRAN was developed by the Air Force Research Laboratory as a way to calculate path radiance and path transmittance in the infrared, visible, and near ultraviolet spectral regions for a given atmospheric path below 100 km. MODTRAN is a band model that uses empirically derived data to compute transmittance and radiance values. SHARC3 is a non-Local Thermodynamic Equilibrium (NLTE) code for computing infrared path radiance for arbitrary paths between 50 and 300 km in the 2 - 40 micron spectral region. It also incorporates SHARC Atmospheric Generator (SAG). SAG is an AFRL code that calculates atmospheric profiles based on geophysical and geographical information. SAG uses the NRL climatological database (PLEXUS, 1999), which is comprised of atmospheric profiles of mean monthly concentrations at 1 to 5 km increments and ten-degree latitude increments. SAG interpolates between these values and PLEXUS uses the output for SAMM.

2.4 Bomem MR-154 Spectrometer

The Bomem MR-154 Fourier Transform Infrared (FTIR) Spectoradiometer is an instrument capable of obtaining highly accurate spectral features of a target source in the 525 cm^{-1} to 6000 cm^{-1} ($19\text{ }\mu\text{m}$ to $5.55\text{ }\mu\text{m}$) range with a maximum resolution of 1 cm^{-1} . The MR-154 FTIR spectrometer is comprised of two subsystems: the data processing and control assembly and a Michelson interferometer.

The data processing and control system consists of a personal computer, which runs the Research Acquire software package. The software package provides a user interface to control the interferometer to collect data. The software also allows a user to process the data to produce calibrated radiance files.

Figure 2.3 is a top view of the interferometer with the main components identified. The main components consist of two detectors, a collimator with an aperture, transfer optics with apertures and a cold subtraction source. The interferometer's two detectors are the mercury, cadmium, and telluride, MCT, a solid-state detector and the indium antimonide, InSb, a solid-state detector. The MCT detector allows for the collection of radiometric data in the 525 cm^{-1} to 1800 cm^{-1} ($19\text{ }\mu\text{m}$ to $5.55\text{ }\mu\text{m}$) region. The InSb detector allows for the collection of radiometric data in the 1800 cm^{-1} to 6000 cm^{-1} ($5.56\text{ }\mu\text{m}$ to $1.67\text{ }\mu\text{m}$) region. The cold subtraction source and the detectors are filled with liquid nitrogen to reduce the thermal noise of the instrument. The collimator and transfer optics, along with their apertures, control the radiometric data reaching the detectors.

Figure 2.4 is reproduced from Hauser (1999). It displays the principle of operation of the FTIR spectrometer. Source radiation enters the spectrometer through the input collimator (1). Then radiation is split by a beam splitter, with one beam reflected by a stationary mirror while, the other's path length is varied with a moving mirror (D1). Then the radiation beam is recombined (2) and recorded as an interferogram.(3) A Fourier transform is applied to the interferogram to produce a raw spectrum (4). The raw spectrum is calibrated using a previously determined calibration spectrum (5). The final output is calibrated spectral data (6). Further information on the components of the

Bomen MR-154 FTIR Spectoradiometer and its operation can be found in the Bomen
MR Series Documentation set (BOMEM Inc. 1997).

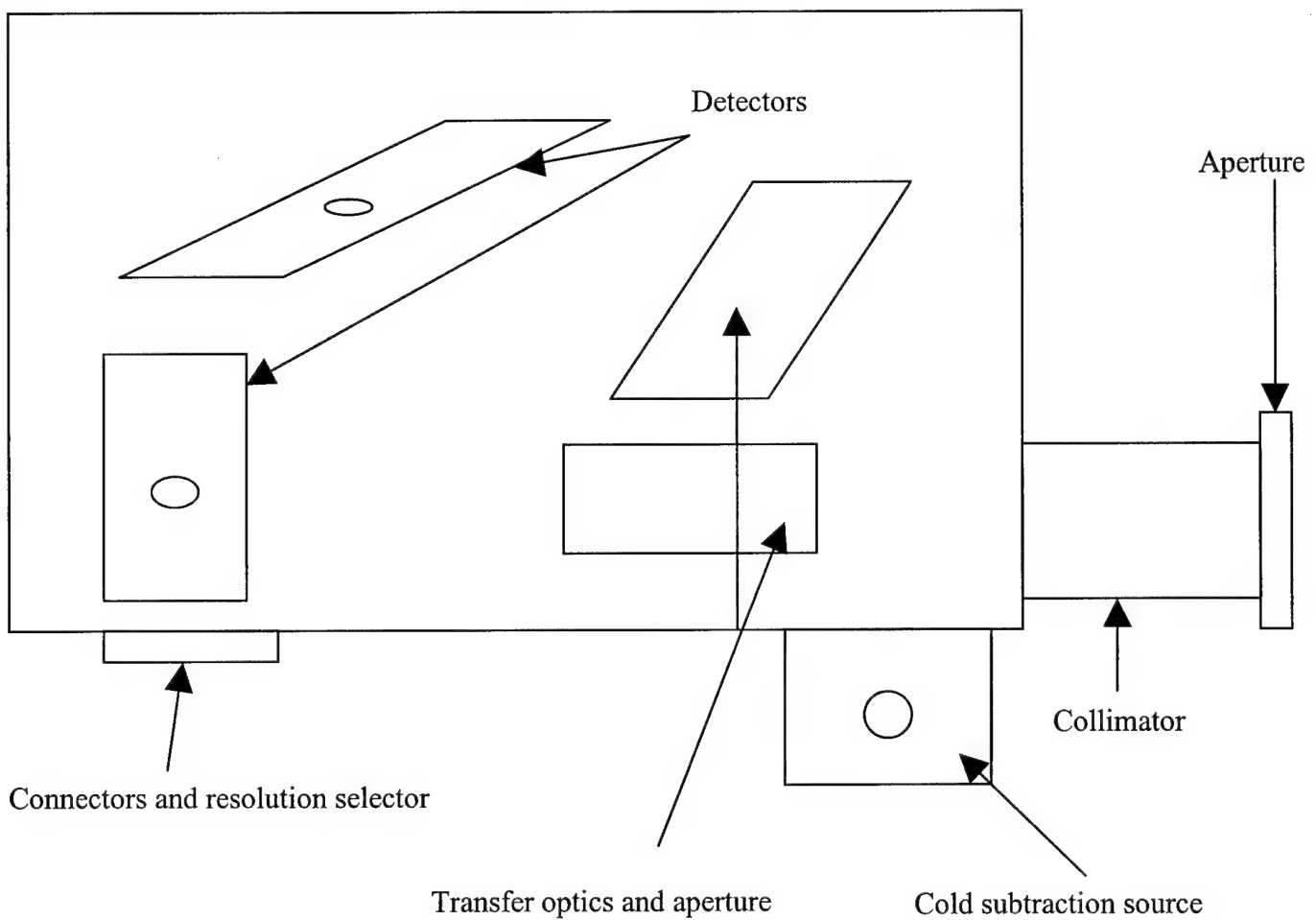


Figure 2.3 Bomen MR-154 Basic Components.

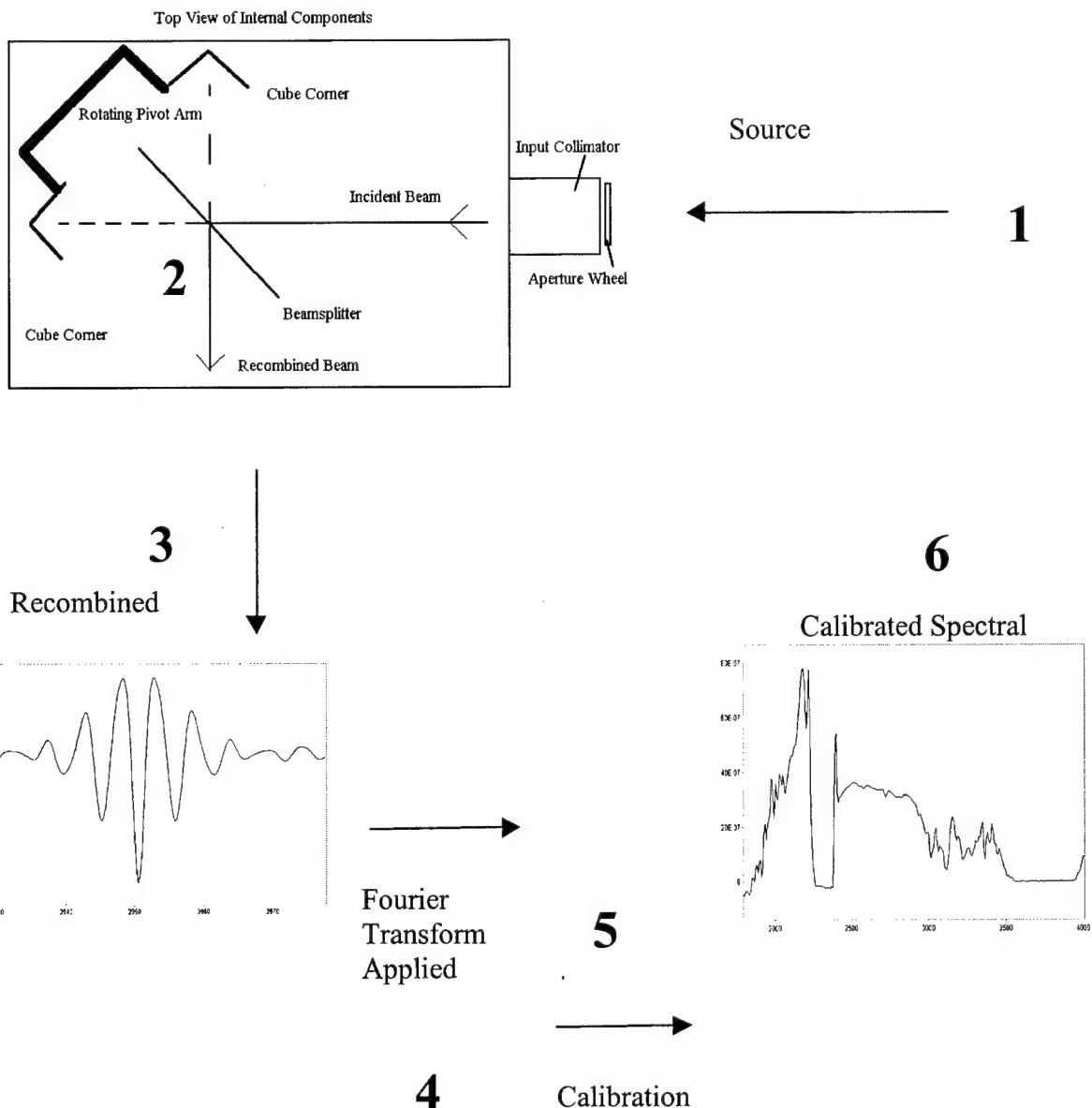


Figure 2.4. Principle of operation of the FTIR spectrometer. Incident energy, 1, aperture and encounters beam splitter at point 2. The beam is recombined where and destructive interference result represented by the interferogram at 3. A Fourier is applied to the interferogram and a raw spectrum results. At 5, a calibration completed. Finally, a calibrated spectral plot is obtained at point 6 (after BOMEM Users Manual.) (Hauser, 1999).

III. Methodology

3.1 Overview

This chapter presents the methodology used during the research. Starting with Equation 2.2, Schwarzschild's equation for the actual radiance is:

$$L_1 = \int W_1(Z)B_1(z)dz \quad (3.1)$$

where,

L_1 = Monochromatic radiation for a specific wavelength of the atmosphere
(W/cm² cm⁻¹ sr⁻¹)

$W_1(z)$ = Kernel function for a specific wavelength of the atmosphere

$B_1(z)$ = Brightness temperature function for a specific wavelength of the atmosphere (W/cm² cm⁻¹)

z = height (meters)

A second radiation equation is employed as a reference:

$$L_2 = \int W_2(Z)B_2(z)dz \quad (3.2)$$

where,

L_2 = Monochromatic radiation for a specific wavelength from an atmospheric model (W/cm² cm⁻¹ sr⁻¹)

$W_2(z)$ = Kernel function for a specific wavelength from an atmospheric model

$B_2(z)$ = Brightness temperature function for a specific wavelength from an atmospheric model (W/cm² cm⁻¹)

Subtracting Equation 3.2 from Equation 3.1 provides a relationship between the atmospheric model derived parameters and the atmospheric parameters.

$$L_1 - L_2 = \int W(z)_1 B_1(z) dz - \int W(z)_2 B_2(z) dz \quad (3.3)$$

Assuming

$$B_1(z) = B_2(z) + \Delta B(z) \quad (3.4)$$

using $\Delta B(z)$ = Change in brightness temperature function ($\text{W/cm}^2 \text{ cm}^{-1}$) then:

$$L_1 - L_2 = \int W(z)_1 (B_2(z) + \Delta B(z)) dz - \int W(z)_2 * B_2(z) dz \quad (3.5)$$

Expanding terms and rearranging,

$$L_1 - L_2 = \int W_1(z) B_2(z) dz + \int W(z)_1 \Delta B(z) dz - \int W(z)_2 * B_2(z) dz \quad (3.6)$$

$$L_1 - L_2 - \int W_1(z) B_2(z) dz + \int W(z)_2 * B_2(z) dz = \int W(z)_1 \Delta B(z) dz \quad (3.7)$$

If the kernel functions, $W(z)$, that do not change with time can be found, that is $W_1(z) = W_2(z)$ then,

$$L_1 - L_2 = \int W(z) \Delta B(z) dz \quad (3.8)$$

In this research, W , L_2 and B_2 are determined using PLEXUS and its integrated atmospheric model, SAMM1. L_1 is actual radiometric measurements using the Bomem MR-154 spectrometer.

We construct an algorithm to find the temperature from the radiometric measurements.

Step 1. We first search regions of the spectrum where the kernel functions are insensitive to the state of the atmosphere while there is a significant change in the observed radiance (see Section 3.2).

Step 2. Kernel functions are calculated using the PLEXUS atmospheric model. The kernel functions will be determined by calculating the transmittance at a number of specified altitudes and then determining the path derivatives $d\tau/dz$ (see Section 3.3).

Ideally, the kernel functions should be continuous, because the change in transmittance is continuous in the atmosphere. The kernel functions calculated with PLEXUS are discrete. For this reason, continuous functions are fitted to the discrete kernel values (see Sections 3.3 and 3.4)..

PLEXUS uses predetermined atmospheric profiles to calculate radiance outputs. Kernel functions were tested by comparing a recovered temperature profile, using the PLEXUS radiance output and previously determined kernel functions, to the model input temperature profile.

Step 3. The final step is to use the spectrometer to recover actual radiance measurements of the atmosphere and determine the temperature profile using the calculated kernel functions. This resulting temperature profile will be compare to a local radiosonde-recovered temperature profile coincident in time (see Sections 3.5 and 3.6)..

3.2 Spectral Region Determination

Spectral regions from 500 cm^{-1} to 3000 cm^{-1} were chosen based on the Bomem spectrometer's spectral range. To minimize the number of possible wavelengths, regions of the spectrum were disqualified as being poor choices for recovering temperature profiles. The first was to disqualify all regions whose absorption is mainly due to highly variable density profiles of atmospheric constituents. Goody and Yung (1989) list three constituents as variable or highly variable and give the appropriate absorption bands associated with the constituents. Table 3.1 lists these constituents and their absorption

bands. These absorption bands were disqualified. Disqualifying these absorption bands leaves the band from 2400 cm^{-1} to 2800 cm^{-1} .

Table 3.1 Highly Variable Atmospheric Constituents and their Absorption Bands.

Constituent	Absorption Band	Transition
H ₂ O, water	$0 \sim 1000\text{ cm}^{-1}$	rotational
H ₂ O, water	$900 \sim 2400\text{ cm}^{-1}$	vibrational
H ₂ O, water	$2800 \sim 4400\text{ cm}^{-1}$	vibrational
O ₃ , ozone	$1000 \sim 1100\text{ cm}^{-1}$	vibrational
CO, carbon monoxide	$2100 \sim 2400\text{ cm}^{-1}$	vibrational

Two dates were chosen based on the National Research Laboratory, NRL, data base temperature profiles. These temperature profiles were used as the inputs to PLEXUS. The months of January and July were chosen based on the greatest differences in the temperature profiles. PLEXUS software was used to calculate radiance value for 650 cm^{-1} to 3000 cm^{-1} . Figure 3.1 is the PLEXUS derived January radiance profile, while Figure 3.2 is the PLEXUS derived July radiance profile. The values are calculated for a path length of infinity, the total atmosphere. Figure 3.3 is the ratio of the two PLEXUS derived radiance profiles.

Transmittance values were calculated using PLEXUS over the 650 cm^{-1} to 3000 cm^{-1} range for both January and July. At each discrete height, the quotients of the July and January transmittance values were determined. Wavenumbers where the quotients were one or near one and there was a significant change in the radiance were considered

to be caused by mostly temperature changes in the input atmospheric profiles. Figure 3.4 displays the ratio of the January and July transmittance values calculated for a path length of the entire atmosphere.

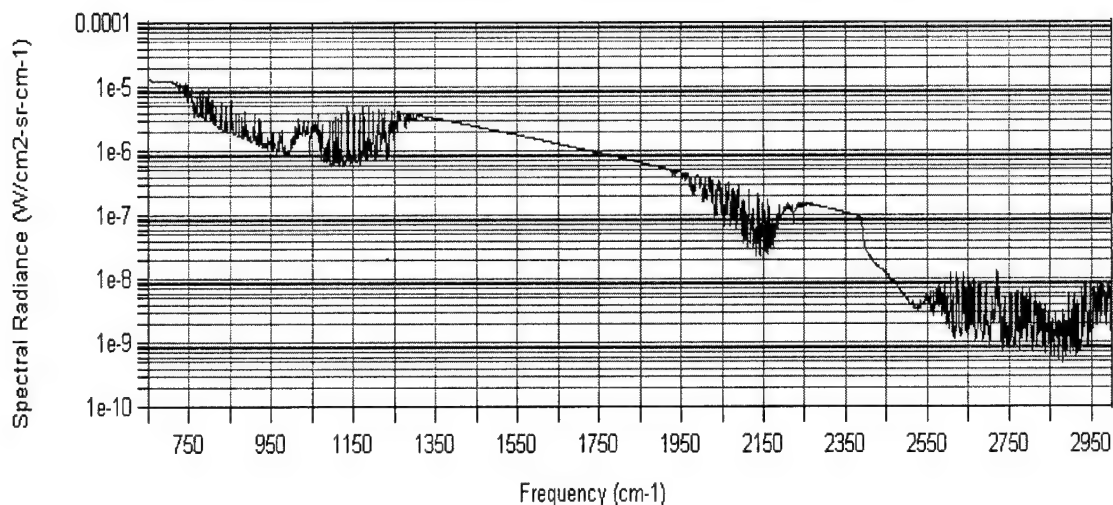


Figure 3.1 PLEXUS graphical radiance output for 15 January 2000.

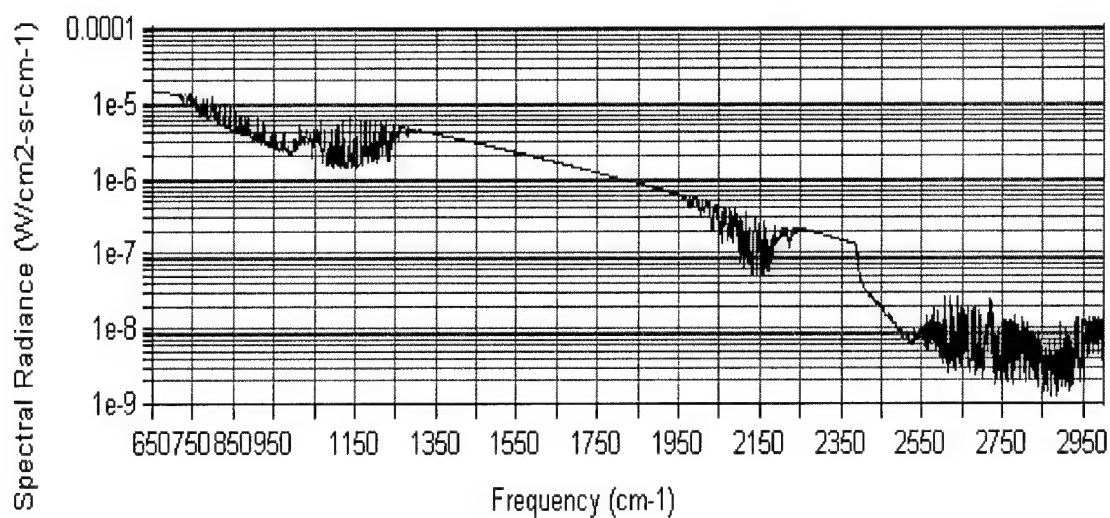


Figure 3.2 PLEXUS graphical radiance output for 15 July 1999.

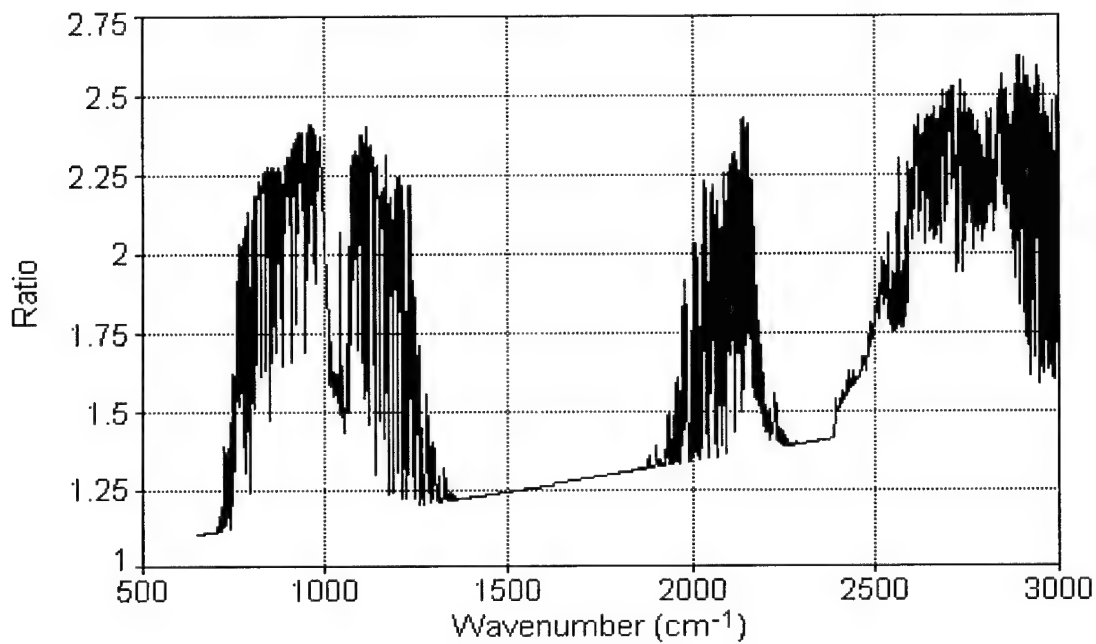


Figure 3.3 Ratio of 15 July 1999 and 15 January 2000 radiances.

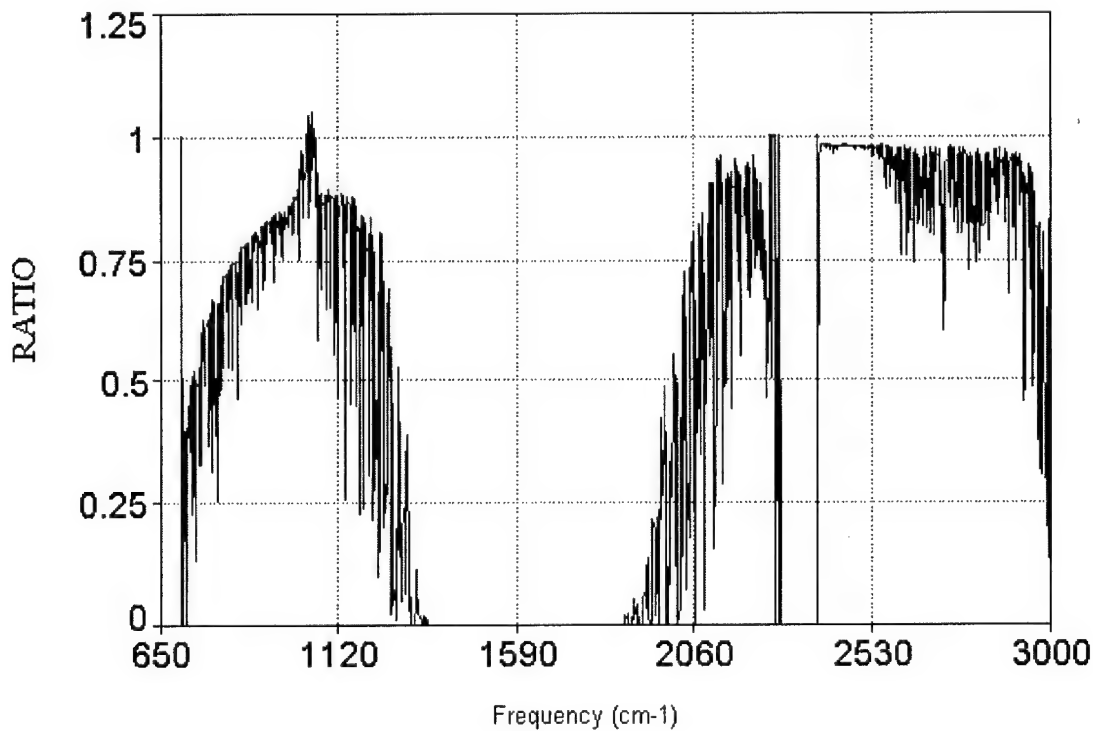


Figure 3.4 Ratio of 15 January 2000 and 15 July 1999 transmissivity.

3.3 Calculating Kernel Functions

PLEXUS was used, in a batch mode, see Appendix 2, to calculate transmittance values over the 650 cm^{-1} to 3000 cm^{-1} range with varying pathlengths. The following pathlengths were used, see Table 3.2..

Table 3.2 Pathlengths used in calculation of transmittance.

Lower Height	Upper Height	Change in Pathlength
0 meters	2 kilometers	10 meters
2 kilometers	10 kilometers	50 meters
10 kilometers	50 kilometers	1000 meters
50 Kilometers	300 kilometers	5000 meters

For selected wavenumbers, the following equation form, Equation 3.9, was calculated by a best-fit software package to fit a function to the discrete transmittance values.

The equation form, Equation 3.10, was used for all calculated transmittance functions, $\tau(z)$ as a function of height, z .

$$\tau(z) = \frac{a + cz}{1 + bz + dz^2} \quad (3.9)$$

Next, the derivative of transmittance with respect to height, that is, the kernel function, was determined. Equation 3.14 shows the derivative of $\tau(z)$ and was used for all used for all calculated kernel functions, W .

$$W(z) = d\tau(z)/dz = \frac{-(-c + cdz + ab + 2adz)}{(1 + bz + dz^2)^2} \quad (3.10)$$

The parameters for the transmittance and kernel functions calculated can be found in Appendix 1.

The following is an example of the method used to determine the kernel functions. Table 3.3 is an example of transmittance values at given heights. Figure 3.5 is the output from the best-fit software using data from Table 3.3.

Table 3.3 Example of transmittance values for specific pathlengths.

Path Length (m)	Transmittance
0	1.000000
100	0.816010
200	0.714550
300	0.642030
400	0.584930
500	0.538240
600	0.499040
700	0.465520
800	0.436640
900	0.411210
1000	0.389160

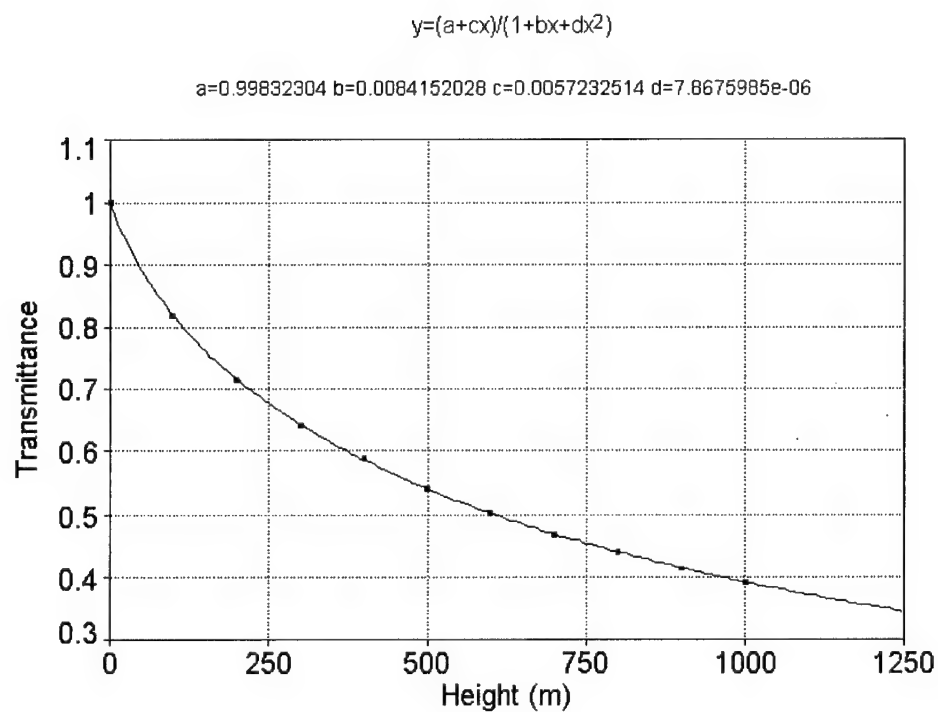


Figure 3.5. Example of output from best-fit software using values from Table 3.3.

3.4 Calculating Atmospheric Brightness Temperature Functions

Atmospheric brightness temperatures were calculated using Planck's formula and physical temperature provided by the atmospheric model. Temperatures from the PLEXUS software were given at discrete height values, see Figure 3.6.

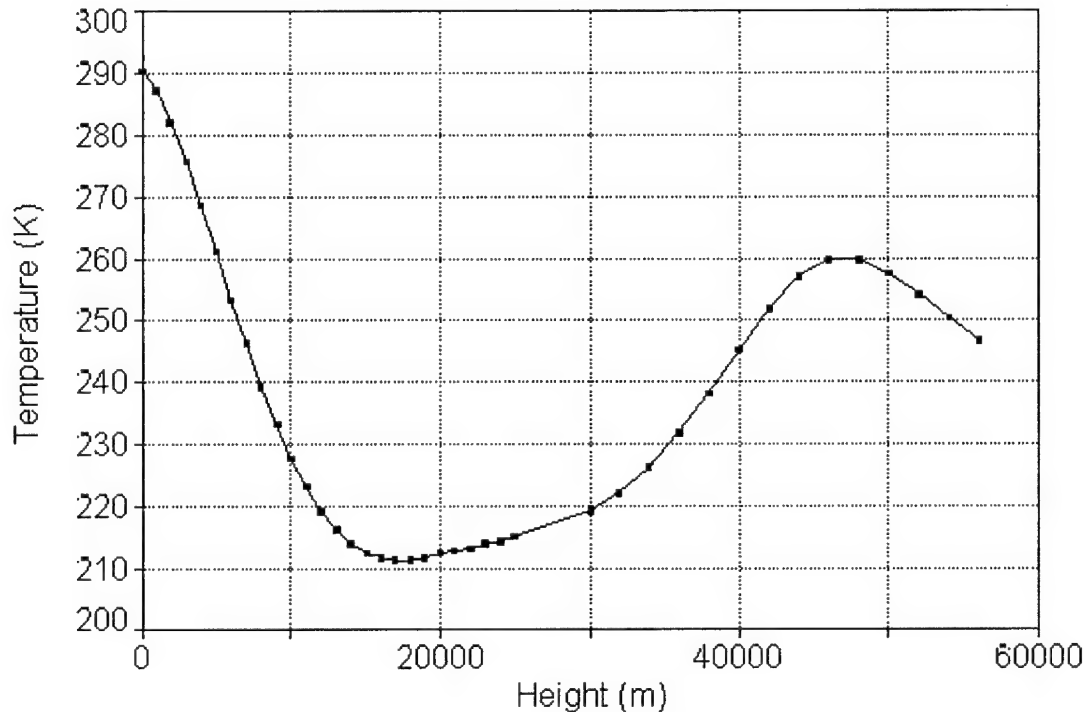


Figure 3.6 Temperature profile used by PLEXUS for 15 November 1999.

These temperature values were used to calculate the brightness temperature at specific wavelengths using Planck's law.

$$B_\lambda = C_1 \lambda^{-5} / [\exp(C_2 / \lambda T) - 1] \quad (3.11)$$

where,

B_λ = brightness temperature ($\text{W/cm}^2 \text{ cm}^{-1}$)

T = temperature (Kelvin)

λ = wavelength (meters)

$$C_1 = 1.1919439 \times 10^{-16} \text{ W m}^2$$

$$C_2 = 1.438769 \times 10^{-2} \text{ m}$$

Once the discrete brightness temperature profile is determined, a best-fit software is used to fit a function to the data. The brightness temperature function calculated for this research can be found in Appendix 1.

The following is an example of the method used to determine the brightness temperature functions. Table 3.4 is an example of calculated brightness temperature at given heights and temperatures using a wavelength of 2568 cm^{-1} . Figure 3.7 is the output from the best-fit software using data from Table 3.4.

Table 3.4 Example of temperature and calculated brightness temperatures for 2568 cm^{-1} .

Height (m)	Temperature (K)	Brightness Temperature ($\text{W/cm}^2 \text{ cm}^{-1}$)
0	290.2	3.91E-07
1000	286.9	3.38E-07
2000	281.9	2.68E-07
3000	275.6	1.98E-07
4000	268.4	1.39E-07
5000	260.9	9.34E-08
6000	253.4	6.12E-08
7000	246.0	3.96E-08
8000	239.2	2.57E-08
9000	232.9	1.70E-08
10000	227.4	1.16E-08
11000	222.8	8.27E-09
12000	219.0	6.20E-09
13000	216.0	4.89E-09
14000	213.7	4.07E-09
15000	212.1	3.58E-09
16000	211.3	3.34E-09
17000	211.0	3.26E-09
18000	211.1	3.29E-09
19000	211.4	3.39E-09
20000	211.9	3.53E-09

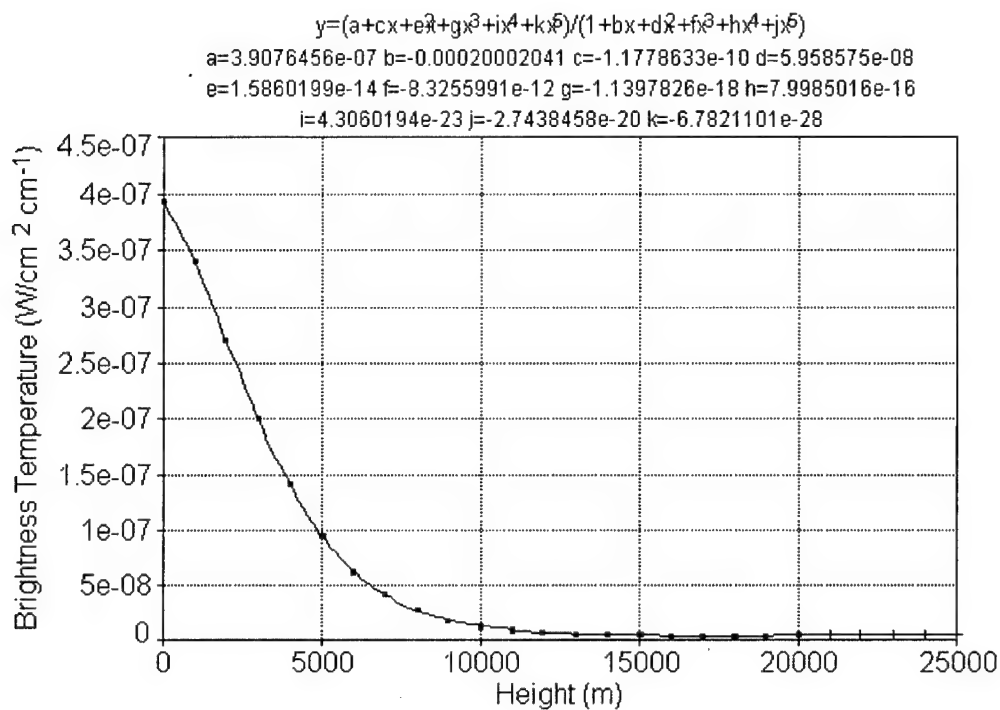


Figure 3.7 Best-fit brightness temperature function using Table 3.4 data.

3.5 Collecting Atmospheric Radiance Measurements

The MR-154 spectrometer was used to obtain atmospheric radiance measurements. The following sections details the setup of the equipment, equipment calibrations and the recovering of atmospheric radiance values.

3.5.1 Spectrometer Setup

The setup of the MR-154 spectrometer was conducted following the procedures in the Bomem MR Series Documentation Set (1997). The MR-154 spectrometer's was deployed on the rooftop of Bldg 640 at Wright-Patterson AFB. The spectrometer's tripod was set up and leveled using the bubble-level located on the tripod. Once the tripod was leveled the azimuth was calibrated using a compass. Next the main assembly was attached to the tripod and the cold subtraction source and detectors were attached to the

main assembly. The cold subtraction source and detectors were filled with liquid nitrogen to ensure a minimal thermal noise. The collimator, amplifier and resolution settings were set to the best setting determined by Hauser (1999): the gain was full, the aperture was at diameter of 6.4 mm, and the resolution was 1 cm^{-1} . The cover to the main assembly was attached and the level of the main assembly was rechecked. The main assembly's internal heater was set to 30 C and allowed to reach equilibrium. Finally the optics, a narrow view telescope, was attached to the main assemble. The narrow view telescope is a Cassegrainian telescope with a focal length of 12 cm. It has a narrow field of view of only 5 milliradians or 0.286 degrees. Cabling was connected from the spectrometer to the computer. This completes the set up of the spectrometer.

3.5.2 Spectrometer Calibration

Spectrum calibration was conducted following the procedures in the Bomem MR Series Documentation Set (1997). A blackbody was place in front of the spectrometer's collimator ensuring it filled the equipment's field of view. This essentially eliminated any stray radiance. The blackbody was set to four different temperatures: 0C, 10C, 30C and 50C, and allowed to stabilize at each temperature. Once the black body stabilized, at each temperature, a radiometric reference was obtained. After the radiometric references were obtained, a calibration file was calculated using the Compute Radiance Correction function in the Research Acquire software. This completes the calibration requirements.

3.5.3 Acquiring Atmospheric Radiometric Data

After the setup and calibration of the equipment, acquiring radiometric data is obtained easily. At a selected time, an interferogram is obtained using the spectrometer. A interferogram measurement was comprised the average of 50 scans. After the

interferogram is obtained, no further use of the spectrometer is needed. The Research Acquire software constructs radiance file from the interferogram, then the calibrated reference file is used to calibrate the radiance file. At this point, calibrated radiance measurements can be taken from the output files or from the display screen.

3.6 Computing Atmospheric Temperature Profiles

The key to this method is to determine $\Delta B(z)$, the change in brightness temperatures as a function of height. Once $\Delta B(z)$ is determined it is used to calculate the actual brightness temperatures by following the previous assumption that the actual brightness temperatures are a summation of the brightness temperature used in PLEXUS and a change in the brightness temperature, $B(z)_{\text{actual}} = B(z)_{\text{plexus}} + \Delta B(z)$, where B_{actual} is the physical brightness temperature and B_{plexus} is the brightness temperature used by PLEXUS software. Temperature is calculated from B_{actual} using Planck's Law.

The first step is to calculate the coefficients for $\Delta B(z)$. This is accomplished by using $L_1 - L_2 = \int W(z)\Delta B(z)dz$, see Equation 3.8. $W(z)$ is calculated using PLEXUS derived kernel functions. The change in radiance, $(L_1 - L_2)$, is calculated using spectrometer radiance measurements, L_1 and PLEXUS radiance calculations, L_2 .

The Mathcad templates, calc_profile_2.mcd and calc_profile_3.mcd, see Appendix 2, are used to retrieve the new temperature profiles. Template calc_profile_2.mcd assumed $\Delta B(z) = a + bz$ and template calc_profile_3.mcd assumed $\Delta B(z) = a + bz + cz^2$.

IV. Results

4.1 Introduction

This chapter lists the results observed during the research and the analysis on success of the physical retrieval method employed. First, the results of spectral range determination are presented. Next, the results from the collection of radiometric data are presented. Finally, the results of the method used to recover atmospheric temperature profiles are discussed.

4.2 Spectral Range Determination

Table 4.1 lists the wavenumbers meeting the selection criteria presented in Chapter 3. First, radiance values for frequencies influenced by highly variable atmospheric constituents were eliminated. This disqualified a significant portion of the initial 650 cm^{-1} to 3000cm^{-1} region, hence wavenumbers outside of the 2400 cm^{-1} and 2800 cm^{-1} region were disqualified. Secondly, the maximum change between the July and January transmittance values at all levels was required to be less than five percent. Next, there was to be a significant change between the January and July radiance values. Figure 3.3 was used to subjectively eliminate the region between 2400 cm^{-1} and 2500 cm^{-1} . Finally, kernel functions not equal to zero above 50,000 meters were eliminated. This was done to decrease the require integration of the radiative transfer equation from 0 km - 300 km to 0 km - 50 km.

Of frequencies listed in Table 4.1, a final set of wavenumbers, 2566 cm^{-1} to 2570 cm^{-1} , was chosen because they are the largest set of continuous wavenumbers meeting the criteria. The larger set allows the use of five independent pieces of information, thereby

allowing a choice in the assumed change in brightness temperature function, $\Delta B(z)$, to have up to five coefficients.

Table 4.1 Most promising frequencies.

Wavenumber (cm ⁻¹)	Ratio of January and July Transmissivity values	Height where transmissivity change with Height = 0 (km)	Change in Radiance with height = 0 (km)	Change in Radiance Between July and January (W/cm ² sr cm ⁻¹)
2534	0.96038	50	50	4.1655E-09
2535	0.97145	50	50	3.3583E-09
2536	0.97491	50	50	3.2157E-09
2537	0.97728	50	50	3.0976E-09
2538	0.97460	50	50	3.2201E-09
2539	0.96863	50	50	3.7177E-09
2540	0.97797	50	50	3.0406E-09
2541	0.97816	50	50	3.0577E-09
2542	0.97875	50	50	3.0566E-09
2566	0.97699	50	50	2.5064E-09
2567	0.97666	50	50	3.2534E-09
2568	0.97922	50	50	2.7339E-09
2569	0.97636	50	50	2.9552E-09
2570	0.95690	50	50	4.2404E-09
2609	0.96152	50	50	2.5490E-09
2610	0.96925	50	50	2.0221E-09
2611	0.97059	50	50	1.9233E-09
2612	0.96647	50	50	2.1797E-09

4.3 Collecting Atmospheric Radiance Measurements

Table 4.2 is a list of the radiance measurement observed by the employed spectrometer. The dates were chosen for clear, cloudless, night conditions. The time was

chosen to correspond to radiosonde data. The measurements were taken on two dates, 1 December 1999 at 0000Z and 8 December 1999 at 0000Z.

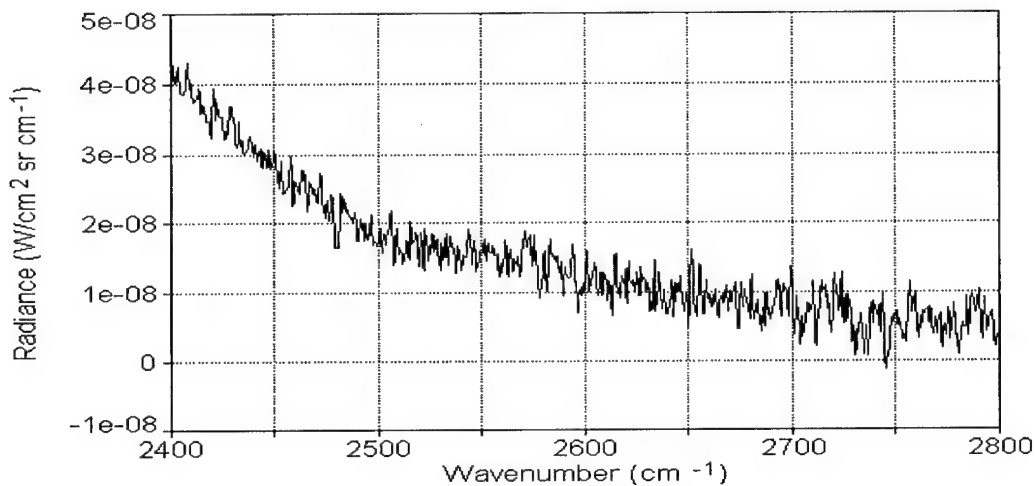


Figure 4.1 Calibrated spectrometer output for 1 December 1999.

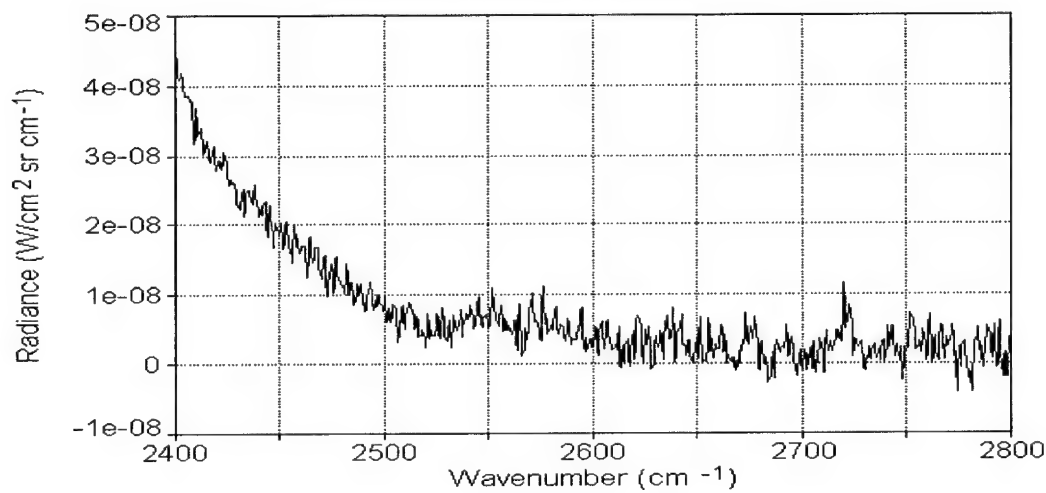


Figure 4.2 Calibrated spectrometer output for 8 December 1999.

Table 4.2 Atmospheric radiance measurements collected by the spectrometer.

Wavenumber (cm ⁻¹)	Measured Radiance Values at 00Z 1 December 1999 (W/cm ⁻² sr cm ⁻¹)	Measured Radiance Values at 00Z 8 December 1999 (W/cm ⁻² sr cm ⁻¹)
2566	1.300 x 10 ⁻⁸	1.721 x 10 ⁻⁸
2567	1.384 x 10 ⁻⁸	1.486 x 10 ⁻⁸
2568	1.491 x 10 ⁻⁸	1.712 x 10 ⁻⁸
2569	1.199 x 10 ⁻⁸	1.621 x 10 ⁻⁸
2570	1.601 x 10 ⁻⁸	1.414 x 10 ⁻⁸

4.4 Computing Atmospheric Temperature Profiles

4.4.1 Test Case I: 1 December 1999

Figure 4.3 and Figure 4.4 display the recovered temperature profile, the radiosonde temperature profile and the temperature profile used in calculating the kernel functions. The spectrometer temperatures in Figure 4.3 were calculated by assuming the form of the change in brightness temperature, $\Delta B(z)$, was $\Delta B(z) = a + bz$. The spectrometer temperatures in Figure 4.4 were calculated by assuming the form of the change in brightness temperature, $\Delta B(z)$, was $\Delta B(z) = a + bz + cz^2$. The retrieval of a temperature profile was successful, although the recovered temperature profile was significantly different than the radiosonde derived temperature profile.

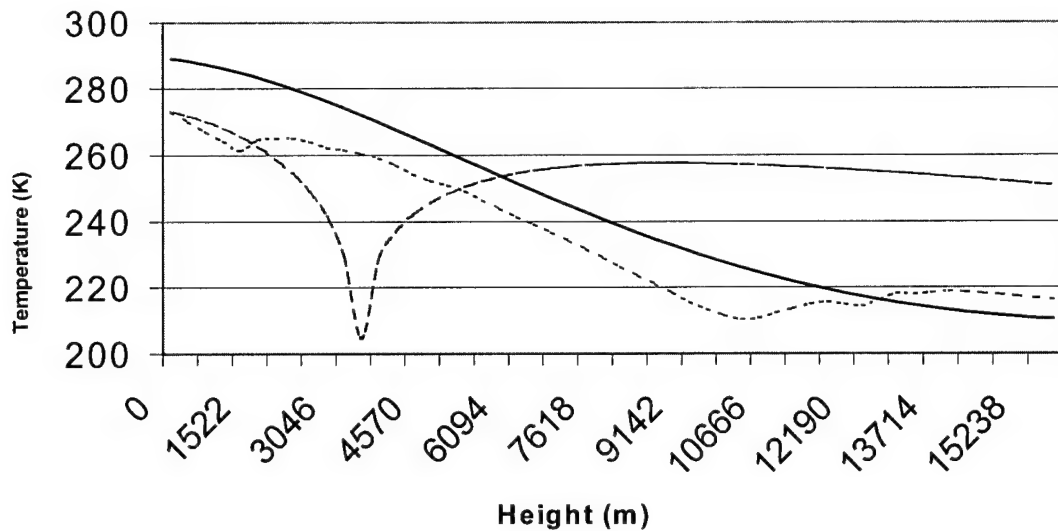


Figure 4.3 Temperature Plots for 1 December 1999.
 Radiosonde Temperatures ___ PLEXUS Temperatures
 - - - Spectrometer Temperatures using $\Delta B(z) = a + bz$.

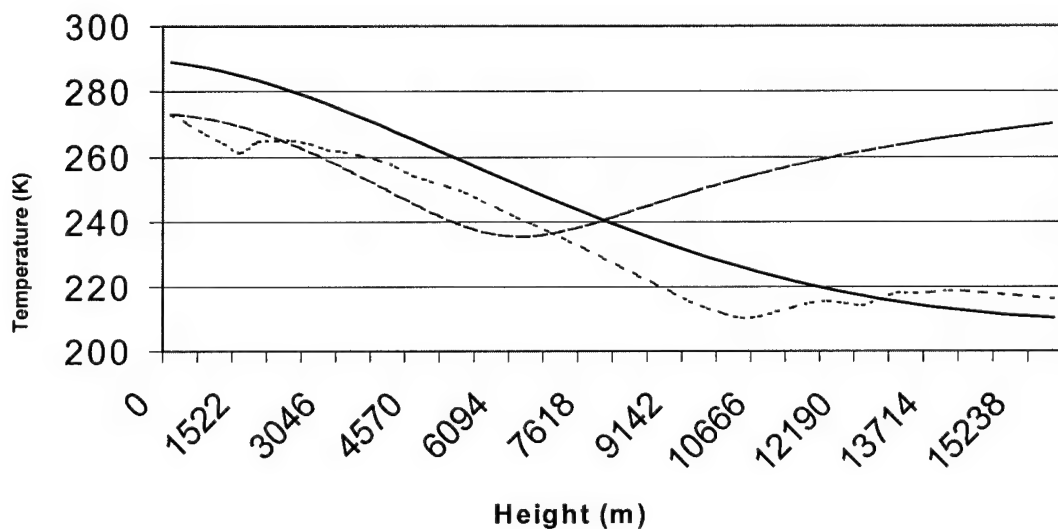


Figure 4.4 Temperature Plots for 1 December 1999.
 Radiosonde Temperatures ___ PLEXUS Temperatures
 - - - Spectrometer Temperatures, using $\Delta B(z) = a + bz + cz^2$.

Figure 4.5 displays $\Delta B(z)$ using radiosonde data and a best-fit function for that data. Figure 4.6 displays plots of $\Delta B(z)$ using radiosonde data , $\Delta B(z) = a + bz$ and $\Delta B(z) = a + bz + cz^2$.

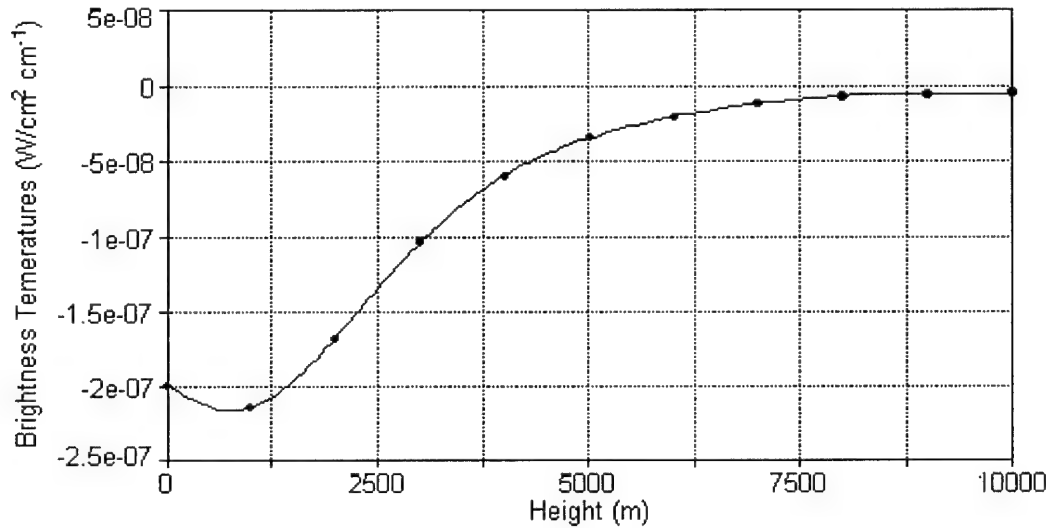


Figure 4.5 Plot of ΔB using 1 December 1999 radiosonde data.

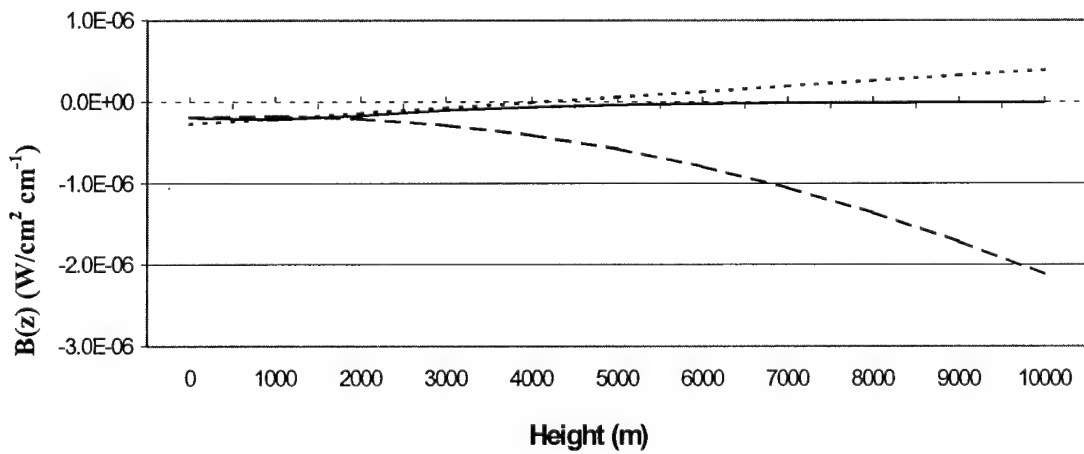


Figure 4.6 Plots of $\Delta B(z)$ for 1 December 1999.
 — $\Delta B(z)$ from radiosonde data $\Delta B(z) = a + bz$ - - - $\Delta B(z) = a + bz + cz^2$.

4.4.2 Test Case II: 8 December 1999

Figure 4.7 and Figure 4.8 display the recovered temperature profile, the radiosonde temperature profile and the temperature profile use in calculating the kernel functions. The spectrometer temperatures in Figure 4.7 were calculated by assuming the form of the change in brightness temperature, $\Delta B(z)$, was $\Delta B(z) = a + bz$. The spectrometer temperatures in Figure 4.8 were calculated by assuming the form of the change in brightness temperature, $\Delta B(z)$, was $\Delta B(z) = a + bz + cz^2$. Similar to test case I, the retrieval of a temperature profile was successful, although the recovery of the radiosonde derived temperature profile was unsuccessful. Figure 4.9 displays ΔB using radiosonde data and a best-fit function for that data. Figure 4.10 displays plots of $\Delta B(z)$ using radiosonde data, $\Delta B(z) = a + bz$ and $\Delta B(z) = a + bz + cz^2$

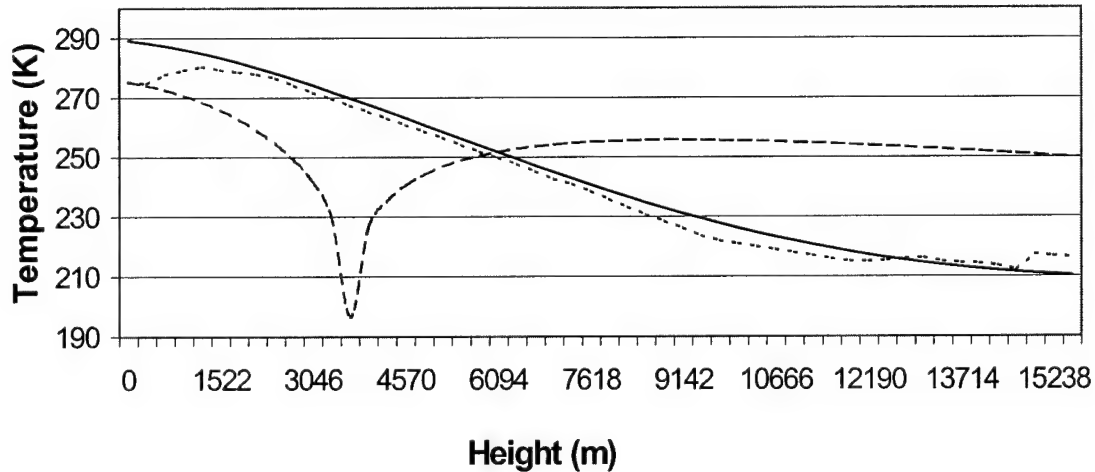


Figure 4.7 Temperature Plots for 8 December 1999.
 Radiosonde Temperatures ___ PLEXUS Temperatures
 - - - Spectrometer Temperatures using $\Delta B(z) = a + bz$.

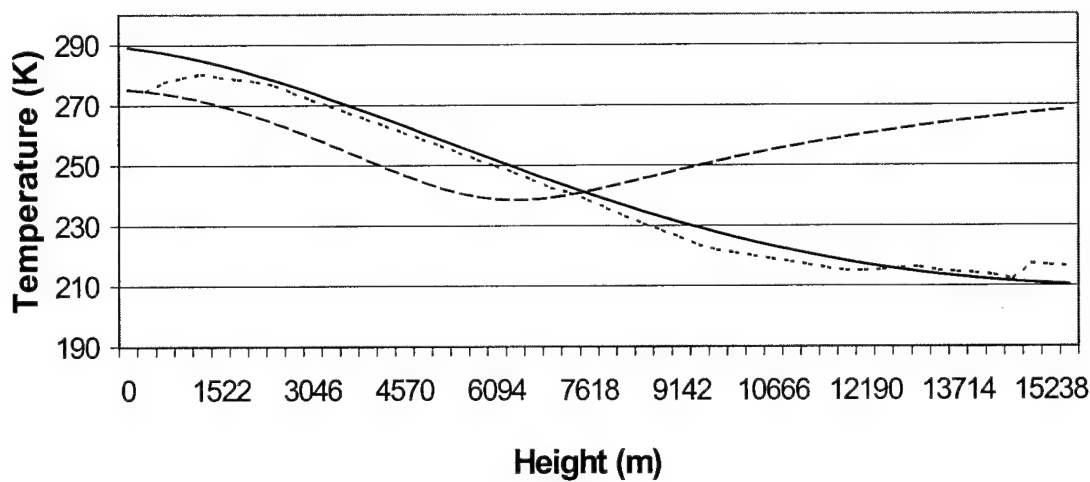


Figure 4.8 Temperature Plots for 1 December 1999.
 Radiosonde Temperatures ___ PLEXUS Temperatures
 - - - Spectrometer Temperatures, using $\Delta B(z) = a + bz + cz^2$.

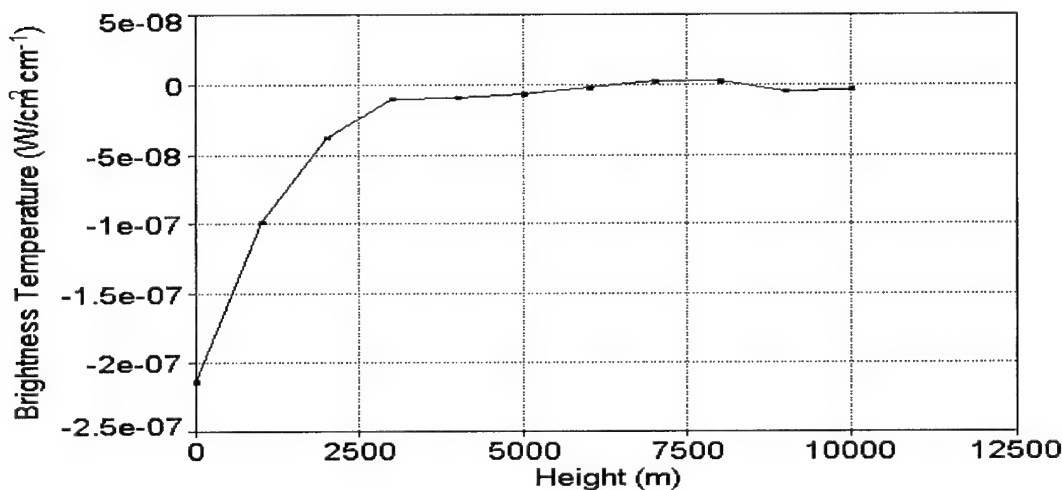


Figure 4.9 Plot of ΔB using 8 December 1999 radiosonde data.

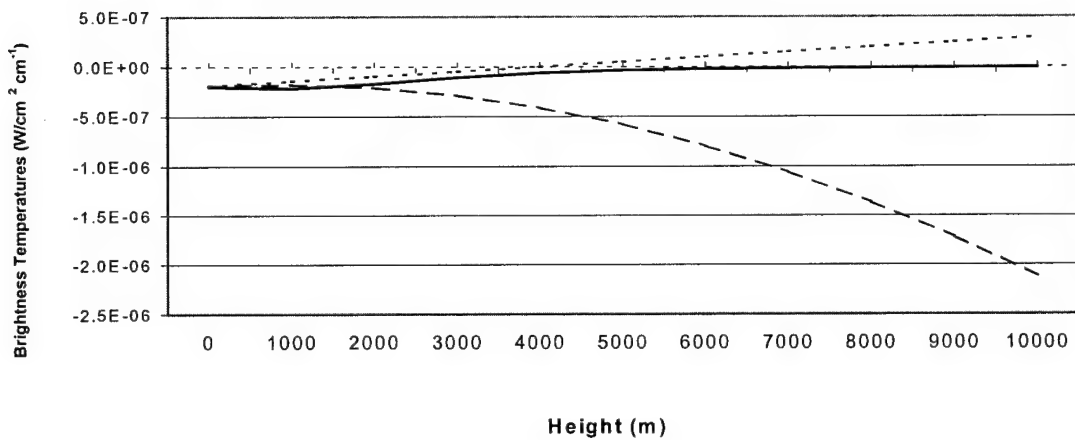


Figure 4.10 Plots of $\Delta B(z)$ for 8 December 1999.

— $\Delta B(z)$ from radiosonde data $\Delta B(z) = a + bz$ - - - $\Delta B(z) = a + bz + cz^2$.

4.4.3 Summary

The fitting of functions to the actual change in brightness temperatures revealed the better form of $\Delta B(z)$ to be a polynomial of higher order than used in this research. Computer precision in calculating the kernel matrix and its inverse limited the choice of assumed forms of $\Delta B(z)$ to no larger than a second-degree polynomial. A qualitative analysis of the recovered temperatures profiles and the assumed forms of $\Delta B(z)$ reveals the assumed form of $\Delta B(z)$ needs to be a higher order polynomial. In both cases, the $\Delta B(z)$ functions using the higher order polynomial produced a temperature profile, which is closer to the radiosonde derived temperature profile for the lower atmosphere.

IV. Conclusions and Recommendations

The method employed in this research was able to recover an atmospheric temperature profile, however significant differences were observe when the recovered temperature profile was compared to a temperature profile recovered by a radiosonde for the same time frame. The investigation of possible choices of frequencies to use in the method revealed various frequencies. Due to the fact that highly variable atmospheric constituents affected the radiance values for most of the initial region, the 2500 cm^{-1} to 2800 cm^{-1} region displayed the most suitable frequencies.

Using functions fitted to model data, kernel and brightness temperature functions, spectral radiances were calculated using Schwarzchild's equation. The calculated spectral radiances did not agree with the spectral radiances calculated from the PLEXUS software. Further research is needed to explain the differences.

The method researched demonstrated its ability to recover an atmospheric temperature profile and I recommend further research of this method. A greater accuracy was observed when the assumed form of $\Delta B(z)$, change in brightness temperature function, used higher order terms. Computer precision limited the assumed polynomial forms of $\Delta B(z)$ to second-degree polynomials. An interesting follow-on research project would be to explore the effects of using different forms for the brightness temperature function, kernel functions, and $\Delta B(z)$ functions and how this affects the accuracy of the recovered temperature profiles. The condition numbers of the matrices are large, on the order of 10^6 , and indicate the matrices may be ill conditioned. The use of different forms for the brightness temperature function, kernel functions and $\Delta B(z)$ may improve the

accuracy of the recovered temperature profile and reduce the condition numbers of the matrices.

In the calibration process, the blackbody's minimum temperature was zero degrees Celsius. This affected the calibration files used by the BOMEM software as minimum atmospheric temperatures are well below zero degrees Celsius. I recommend obtaining a blackbody capable of lower minimum temperatures to use in the calibration process. In verifying the recovered temperatures, the radiosonde and spectrometer sites were approximately thirty miles apart. If possible, the radiosonde and spectrometer sites should be the same to help reduce error.

Appendix 1: Brightness Temperature and Transmittance Function Data

This section contains the best-fit function data for brightness temperature function as well as the transmittance and kernel parameters for 2566 cm^{-1} to 2570cm^{-1} .

Brightness Temperature Data

$B(z) = (a + cz + ez^2 + gz^3 + iz^4 + kz^5) / (1 + bz + dz^2 + fz^3 + hz^4 + jz^5)$ is the function chosen to represent the brightness temperatures used by the PLEXUS software to calculate transmittance and radiance values. Table A.1.1 lists the values and statistical data of the parameters for the equation. The adjusted r^2 value for the fitted equation is 0.99999994.

Table A.1.1 Numeric summary of fitted brightness temperature function parameters.

Parm	Value	Std_Error	t-value	P> t
a	3.90765E-07	4.16314E-11	9386.29893	0.0000
b	-2.00020E-04	4.34230E-06	-46.06311	0.0000
c	-1.17790E-10	1.73953E-12	-67.71151	0.0000
d	5.95852E-08	1.13240E-09	52.61859	0.0000
e	1.58601E-14	3.42736E-16	46.27508	0.0000
f	-8.32550E-12	3.61496E-13	-23.03055	0.0000
g	-1.13980E-18	3.88107E-20	-29.36751	0.0000
h	7.99827E-16	7.85057E-17	10.18815	0.0000
i	4.30596E-23	2.64977E-24	16.25029	0.0000
j	-2.74370E-20	5.37737E-21	-5.10239	0.0005
k	-6.78200E-28	7.27836E-29	-9.31799	0.0000

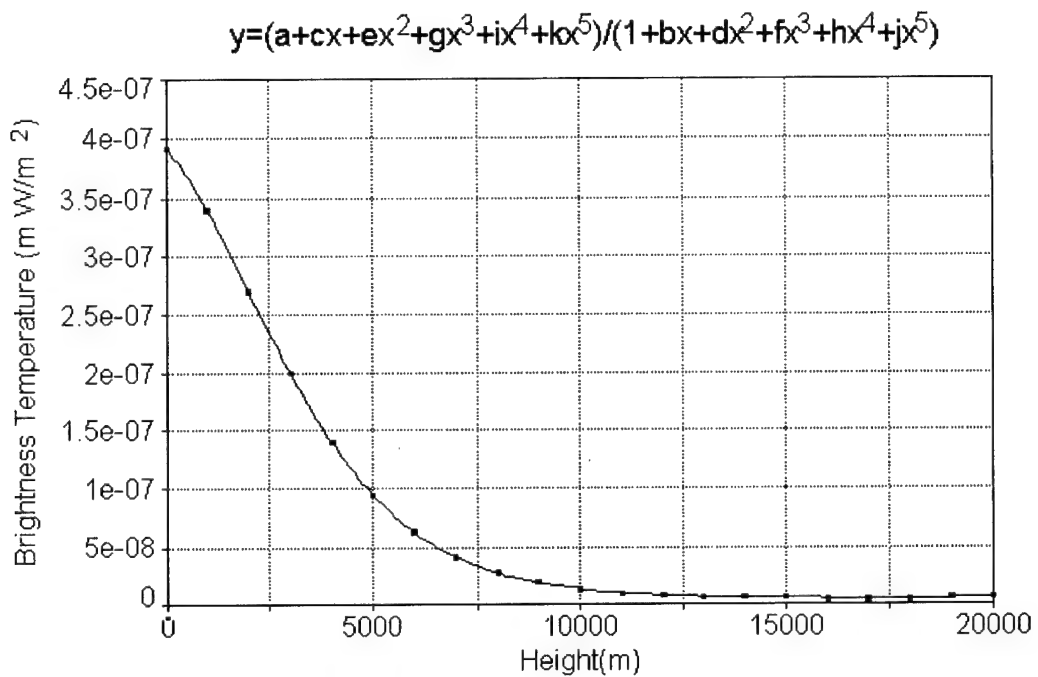


Figure A.1.1 Plot of brightness temperature data points and fitted function.

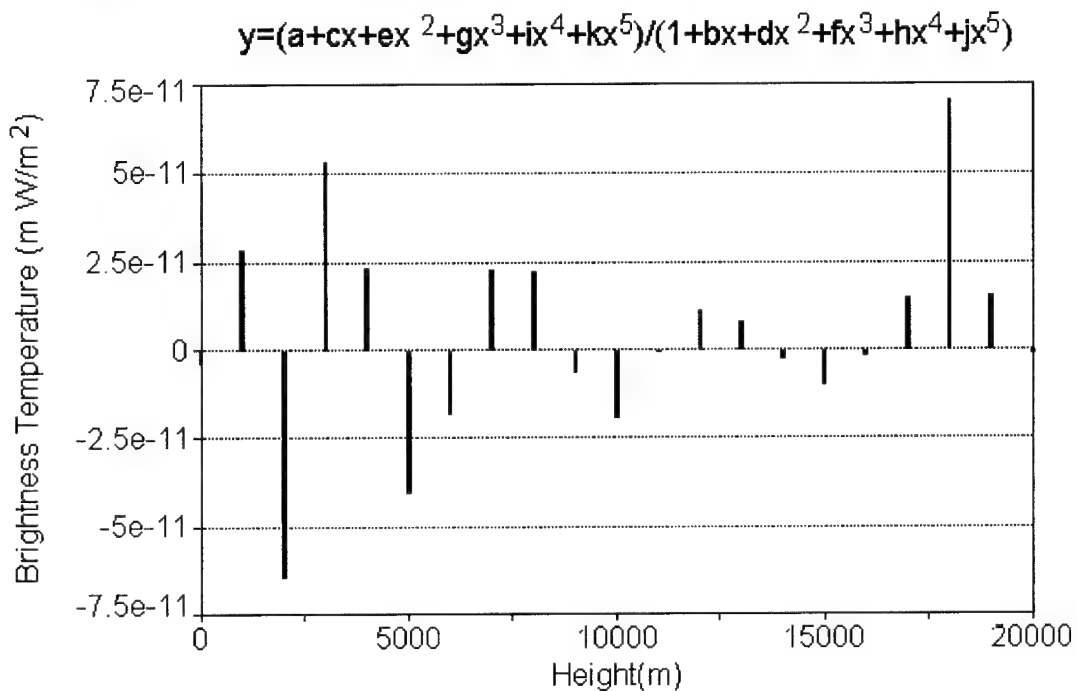


Figure A.1.2 Residual plot of fitted brightness temperature function.

2566 cm⁻¹ Data

$\tau_{2566}(z) = (a + cz) / (1 + bz + dz^2)$ is the function chosen to represent the transmittance values calculated by the PLEXUS software. Table A.1.2 lists the values and statistical data of the parameter for the equation. The adjusted r2 value for the fitted equation is 0.9995.

Table A.1.2 Numeric summary for transmittance and kernel parameters for 2566 cm⁻¹.

Parm	Value	Std_Error	t-value	P> t
a	0.999910333	9.97147e-05	10027.70781	0.0000
b	0.000308564	8.31176e-07	371.2381899	0.0000
c	0.000262176	7.32808e-07	357.7684234	0.0000
d	-1.1198e-10	4.51076e-13	-248.259375	0.0000

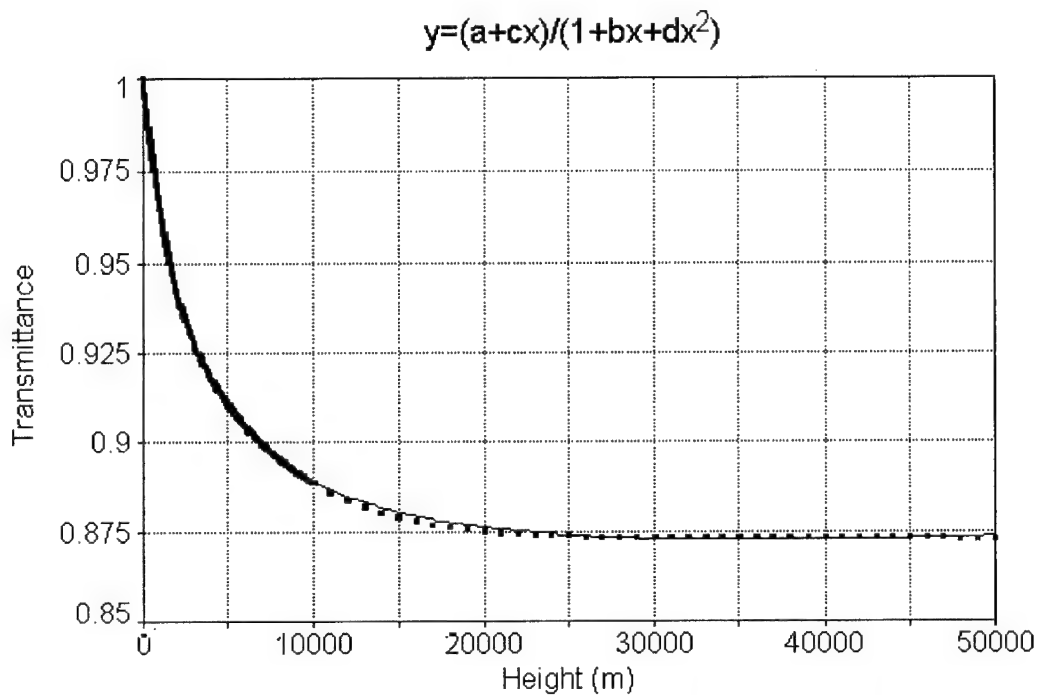


Figure A.1.3 Plot of transmittance values and fitted function for 2566 cm^{-1} .

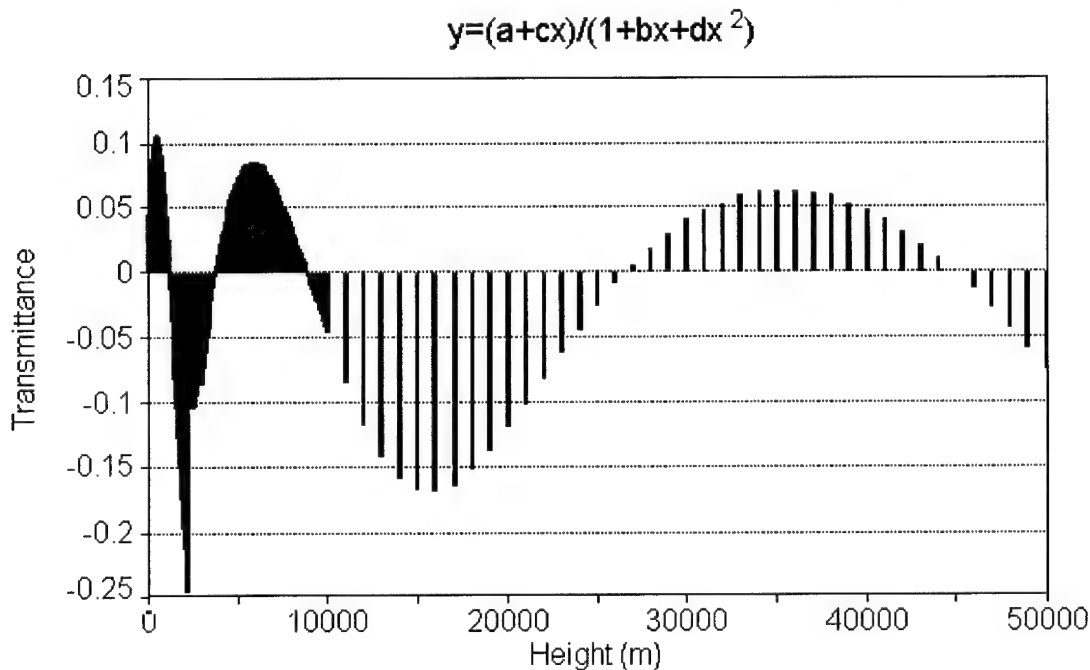


Figure A.1.4 Residual plot of fitted transmittance function for 2566 cm^{-1} .

2567 cm⁻¹ Data

$\tau_{2567}(z)=(a+cz)/(1+bz+dz^2)$ is the function chosen to represent the transmittance values calculated by the PLEXUS software. Table A.1.2 lists the values and statistical data of the parameter for the equation. The adjusted r2 value for the fitted equation is 0.9997224799.

Table A.1.3 Numeric summary for transmittance and kernel parameters for 2567 cm⁻¹.

Parm	Value	Std_Error	t-value	P> t
a	0.998440828	0.00011731	8511.142627	0.0000
b	0.000206724	5.15083e-07	401.3422029	0.0000
c	0.000151993	4.19289e-07	362.500531	0.0000
d	-2.1125e-10	6.49634e-13	-325.190357	0.0000

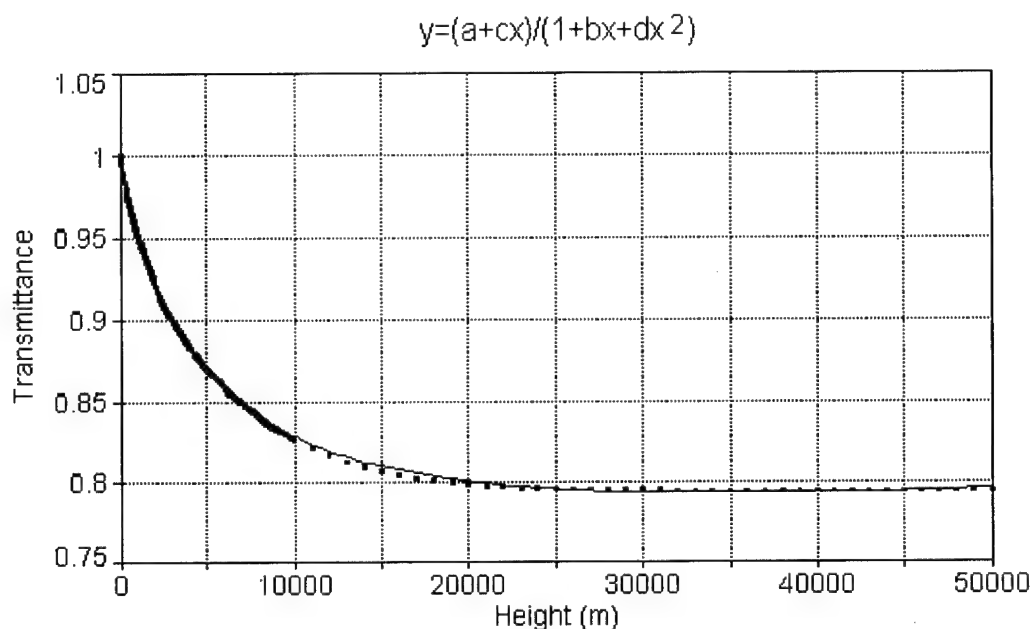


Figure A.1.5 Plot of transmittance values and fitted function for 2567 cm^{-1} .

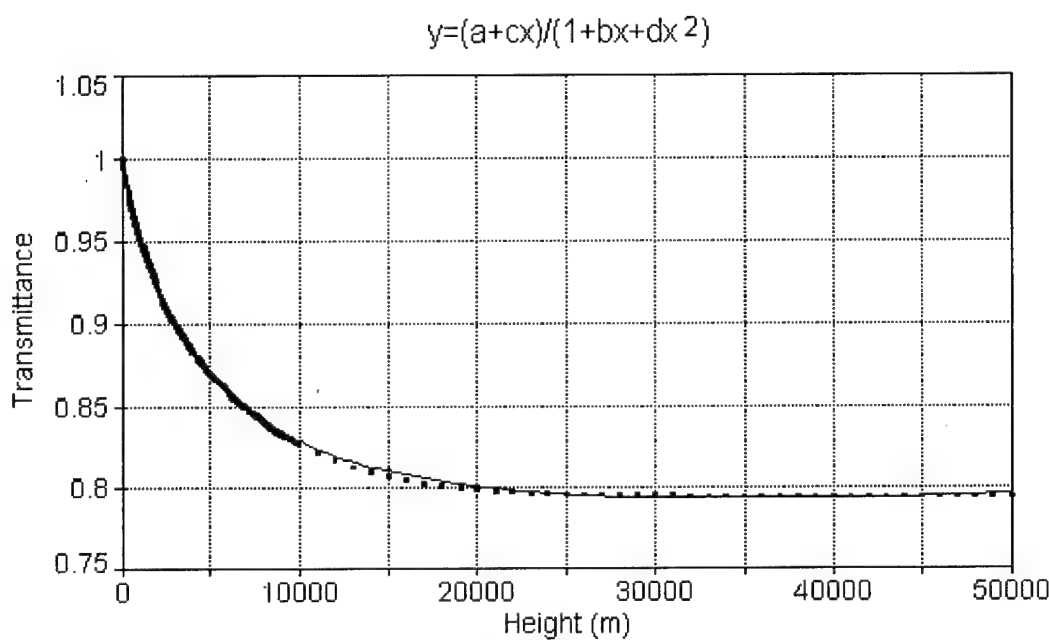


Figure A.1.6 Residual plot of fitted transmittance function for 2567 cm^{-1} .

2568 cm⁻¹ Data

$\tau_{2568}(z) = (a + cz)/(1 + bz + dz^2)$ is the function chosen to represent the transmittance values calculated by the PLEXUS software. Table A.1.2 lists the values and statistical data of the parameter for the equation. The adjusted r² value for the fitted equation is 0.9998.

Table A.1.4 Numeric summary for transmittance and kernel parameters for 2568 cm⁻¹.

Parm	Value	Std_Error	t-value	P> t
a	0.999895747	7.8544e-05	12730.3925	0.0000
b	0.000237587	4.45246e-07	533.6068558	0.0000
c	0.00018786	3.76929e-07	498.3963266	0.0000
d	-1.6576e-10	3.95142e-13	-419.50688	0.0000

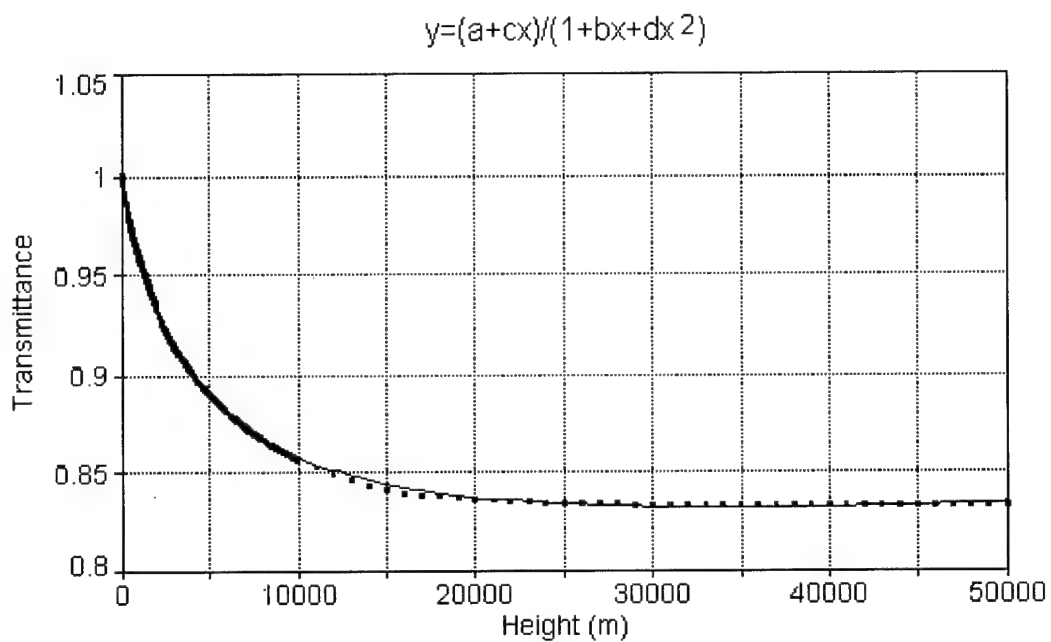


Figure A.1.7 Plot of transmittance values and fitted function for 2568 cm^{-1} .

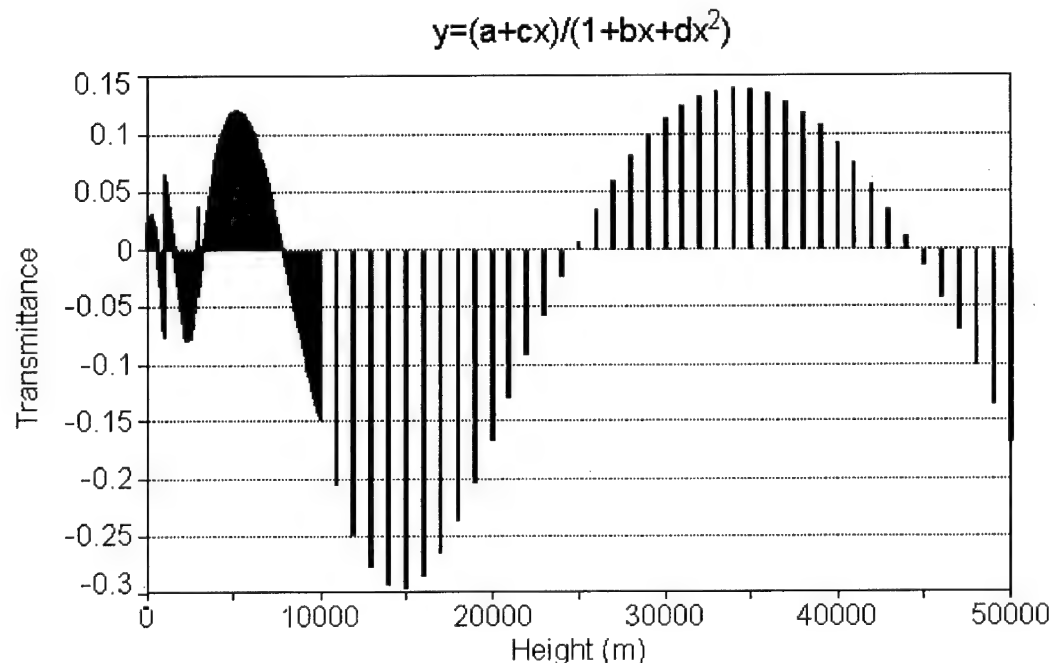


Figure A.1.8 Residual plot of fitted transmittance function for 2568 cm^{-1} .

2569 cm⁻¹ Data

$\tau_{2569}(z) = (a + cz)/(1 + bz + dz^2)$ is the function chosen to represent the transmittance values calculated by the PLEXUS software. Table A.1.2 lists the values and statistical data of the parameter for the equation. The adjusted r² value for the fitted equation is 0.9998292345.

Table A.1.5 Numeric summary for transmittance and kernel parameters for 2569 cm⁻¹.

Parm	Value	Std_Error	t-value	P> t
a	1.000358467	8.185e-05	12221.85763	0.0000
b	0.000243899	4.48959e-07	543.2543509	0.0000
c	0.000190951	3.77011e-07	506.4856435	0.0000
d	-1.7589e-10	4.10406e-13	-428.583981	0.0000

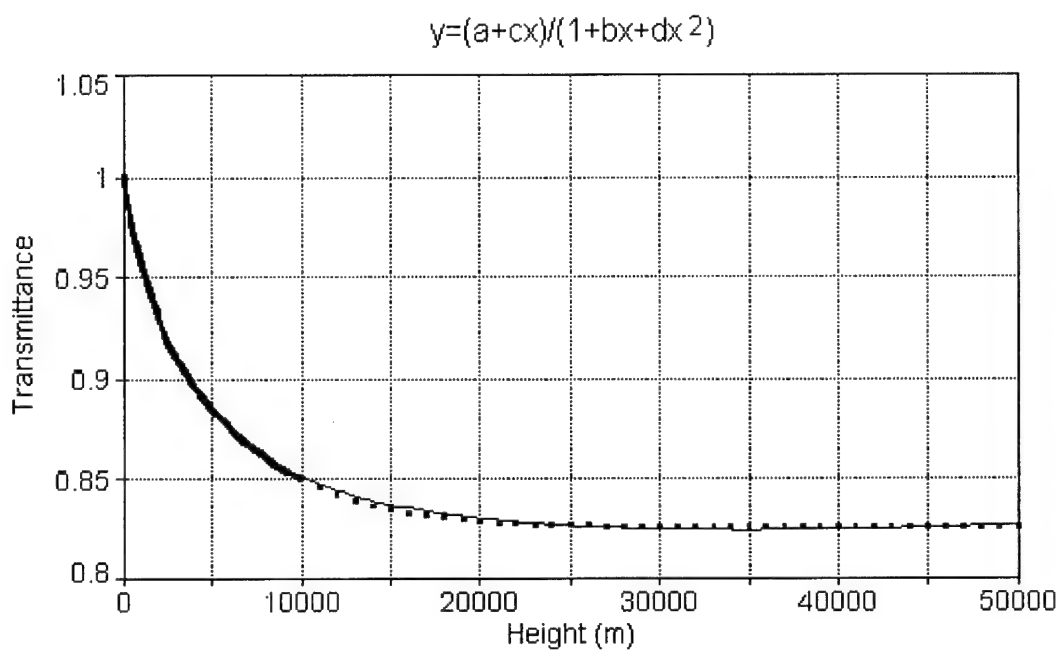


Figure A.1.9 Plot of transmittance values and fitted function for 2569 cm^{-1} .

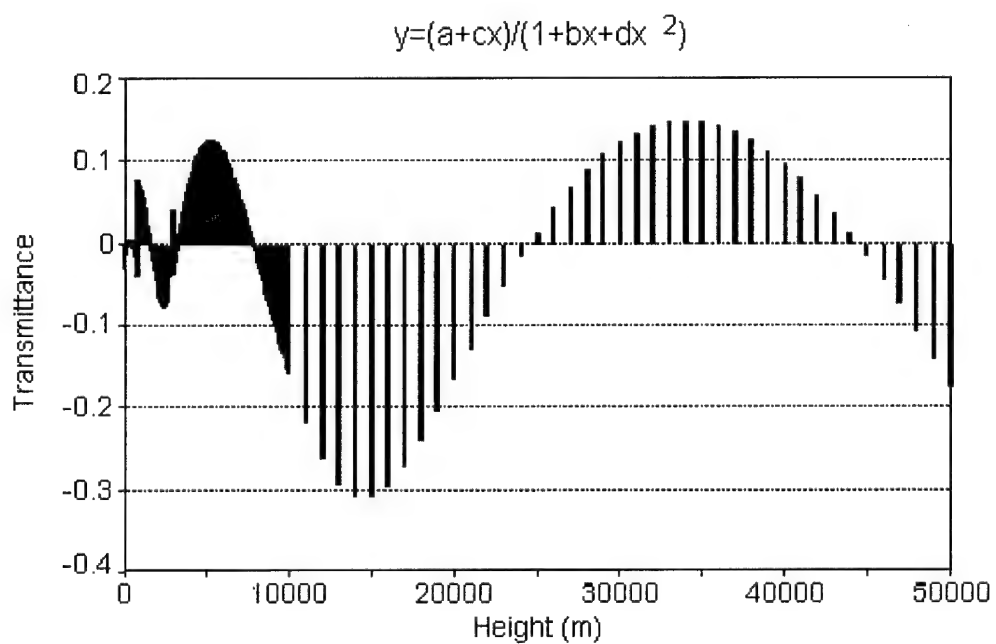


Figure A.1.10 Residual plot of fitted transmittance function for 2569 cm^{-1} .

2570 cm⁻¹ Data

$\tau_{2570}(z) = (a + cz)/(1 + bz + dz^2)$ is the function chosen to represent the transmittance values calculated by the PLEXUS software. Table A.1.2 lists the values and statistical data of the parameter for the equation. The adjusted r² value for the fitted equation is 0.9998559591.

Table A.1.6 Numeric summary for transmittance and kernel parameters for 2570 cm⁻¹.

Parm	Value	Std_Error	t-value	P> t
a	1.001225275	8.88782e-05	11265.13557	0.0000
b	0.000289502	4.53913e-07	637.7904422	0.0000
c	0.000219657	3.69277e-07	594.8294418	0.0000
d	-2.0814e-10	4.35863e-13	-477.529018	0.0000

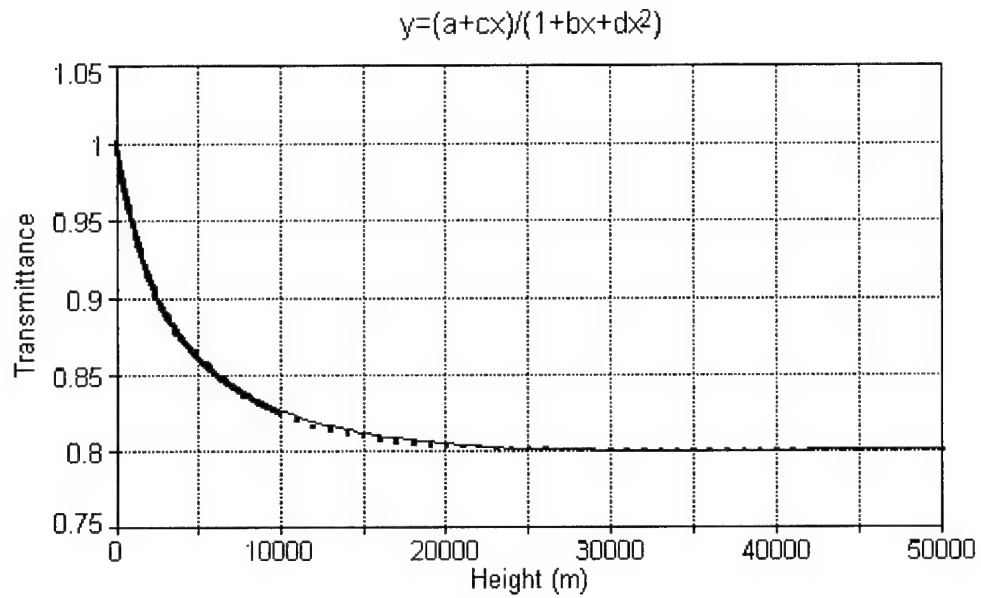


Figure A.1.11 Plot of transmittance values and fitted function for 2570 cm^{-1} .

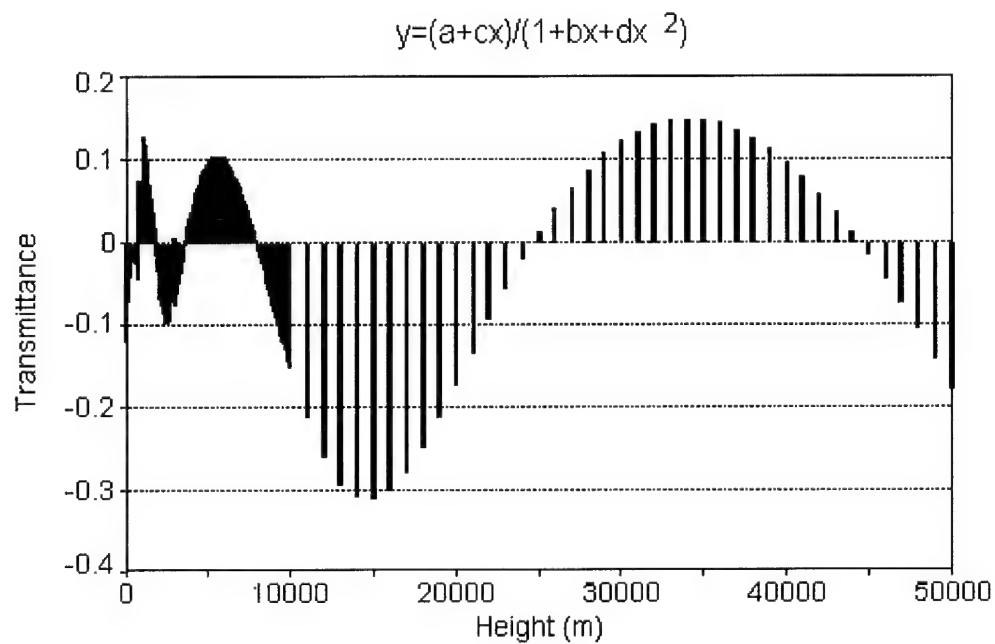


Figure A.1.12 Residual plot of fitted transmittance function for 2570 cm^{-1} .

APPENDIX 2: IDL Programs and Mathcad Templates

Two IDL programs and two Mathcad templates are provided.

The two IDL programs are Plexusbatch.pro and ADI.pro. Plexusbatch.pro increments the pathlengths in the PLEXUS input file then call the PLEXUS program to compute radiance and transmittance value for that pathlength. ADI.pro manipulates PLEXUS outputs. It takes 200 individual transmittance file produced by PLEXUS and put them into one files in a column format for easy importation into Microsoft Excel.

The two Mathcad templates are Recover_Profile_2.MCD and Recover_Profile_3.MCD. Recover_Profile_2.MCD assumes $\Delta B(z) = a + bz$, solves for $\Delta B(z)$ and calculate the a temperature profile. Recover_Profile_3.MCD assumes $\Delta B(z) = a + bz + cz^2$, solves for $\Delta B(z)$, and calculate the a temperature profile.

Plexusbatch.pro

```
pro plexusbatch
```

; This program increments the pathlengths in the PLEXUS input file then call the PLEXUS program to compute radiance and transmittance value for that pathlength.

```
; closes all devices left open  
for j=1,200 do begin ; loop1  
    close,/all
```

;allows selection of a input and output files

```
fm='c:\plexus\data_out\adi\height.txt'  
fn='c:\plexus\adi\adi.cpd'
```

; defines a string variable

```
s=""
```

; returns the number of rows in the file

```
while not (EOF(2)) do begin  
    readf,2,s  
    n=n+1  
endwhile
```

```
;total=n-1
```

```
close,2
```

; read pathlength line of input file

```
openr,2,fn  
lines=strarr(n)  
readf,2,lines  
close,2
```

```
var=j*0.010  
var=strcmp(string(var))
```

```
lines(29)="Final_Altitude="+var+" ;[H2ALT-F,M,S,U] (KM)"
```

```
file_name='c:\plexus\adi\adi.cpd'
file_name2='c:\plexus\data_out\adi\height.txt'
close, /all

; Writes new pathlength line to PLEXUS input file;

openu,2,file_name;,/append
openu,3,file_name2,/append
for i=0l,n-1 do begin
;print, i
    printf,2,lines(i)

; Writes pathlength value to file;

Endfor
printf,3,j,var*100.0
print, 'wrote the file'

close,/all
spawn, 'plexus.exe c:\plexus\adi\adi.cpd'
endfor
```

ADI.PRO

pro adi

; This program takes 200 individual transmittance file produced by PLEXUS and put them into one files in a column format.

; closes all devices left open

close,/all

;allows selection of a specific file

fn='c:\plexus\adi\excel2.out'

```
output=fltarr(20,2351)
for i=0,19 do begin
num=strcompress(sindgen(1000),/remove_all)
num(0:9)='0'+num(0:9)
num(0:99)='0'+num(0:99)
var=num(i+431)
print, var
```

```
fm='E:\15jul99\adi'+var+'.trn'
print, fm
openr,2,fm
data=fltarr(2,2351)
readf,2,data
close,2
output(i,*)=data(1,*)
endfor
openw,3,fn, width=1300
format='(20(E12.5,1x))'
printf,3,output,format=format
close,2
close,/all
end
```

Recover_Profile_2.MCD

ORIGIN=1

This mathcad template calculates a temperature profile assuming the change in the brightness temperature function is $\Delta B(z) := (a_b + b_b \cdot z)$.

Assuming B is linear in form

$$\Delta B(z) := (a_b + b_b \cdot z)$$

Transmittance and kernel functions for 2567 cm⁻¹

$$a_{2567} := 0.99844082$$

$$b_{2567} := 0.00020672$$

$$c_{2567} := 0.00015199$$

$$d_{2567} := -2.112510^{-10}$$

$$\tau_{2567}(z) := \frac{a_{2567} + c_{2567}z}{1 + b_{2567}z + d_{2567}z^2}$$

$$w_{2567}(z) := \frac{-(-c_{2567} + c_{2567}d_{2567}z^2 + a_{2567}b_{2567} + 2 \cdot a_{2567}d_{2567}z)}{(1 + b_{2567}z + d_{2567}z^2)^2}$$

Transmittance and kernel functions for 2568 cm⁻¹

$$a_{2568} := 0.99989574$$

$$b_{2568} := 0.00023758$$

$$c_{2568} := 0.0001878$$

$$d_{2568} := -1.657610^{-10}$$

$$\tau_{2568}(z) := \frac{a_{2568} + c_{2568}z}{1 + b_{2568}z + d_{2568}z^2}$$

$$W_{2568}(z) := \frac{-(-c_{2568} + c_{2568}d_{2568}z^2 + a_{2568}b_{2568}z + 2 \cdot a_{2568}d_{2568}z)}{(1 + b_{2568}z + d_{2568}z^2)^2}$$

Solving for kernel functions coefficients

$$\int_0^{55000} \Delta B(z) \cdot W_{2567}(z) dz \text{ simplify } \Rightarrow - .2007062487288491151a_b - 828.1309354433689600b_b$$

$$\int_0^{55000} \Delta B(z) \cdot W_{2568}(z) dz \text{ simplify } \Rightarrow -.16454915550831362638a_b - 645.6013855647161000b_b$$

Kernel Function Coeff.

$$W := \begin{bmatrix} .2007062487288491151 \\ .16454915550831362639645.6013855647161000 \end{bmatrix}$$

Radiance values for 2567 cm-1 and 2568 cm-1, respectively, from PLEXUS output.

$$L_{plexus} := \begin{bmatrix} 7.48100010^{-9} \\ 6.19910010^{-9} \end{bmatrix}$$

Radiance values for 2567 cm-1 and 2568 cm-1, respectively, obtained using spectrometer.

$$L_{spect} := \begin{bmatrix} 1.386 \cdot 10^{-8} \\ 1.491 \cdot 10^{-8} \end{bmatrix} \cdot \text{weight}$$

Calculating ($L_1 - L_2$)

$$\Delta L_1 := L_{\text{spect}} - L_{\text{plexus}}$$

Radiance difference for 2567 cm⁻¹ and 2568 cm⁻¹, respectively.

$$\Delta L_1 = \begin{bmatrix} -1.0776810^{-9} \\ 6.893200000000000 \cdot 10^{-10} \end{bmatrix}$$

Solving for the change in brightness temperature function, DB(z), coefficients

$$\text{coeff}_1 := W^{-1} \cdot \Delta L_1$$

$$\text{coeff}_1 = \begin{bmatrix} -1.89270218831872 \cdot 10^{-7} \\ 4.71729698117343 \cdot 10^{-11} \end{bmatrix}$$

$$a_b := \text{coeff}_{1_1}$$

$$b_b := \text{coeff}_{1_2}$$

$$a_b = -1.89270218831872 \cdot 10^{-7}$$

$$b_b = 4.71729698117343 \cdot 10^{-11}$$

$$\Delta B_1(z) := a_b + b_b \cdot z$$

Brightness temperature function used to calculate initial kernel functions

$$a_b := 3.90765 \cdot 10^{-7}$$

$$b_b := -2.0002 \cdot 10^{-4}$$

$$c_b := -1.1779 \cdot 10^{-10}$$

$$d_b := 5.95852 \cdot 10^{-8}$$

$$e_b := 1.586 \cdot 10^{-14}$$

$$f_b := -8.3255 \cdot 10^{-12}$$

$$g_b := -1.1398 \cdot 10^{-18}$$

$$h_b := 7.99827 \cdot 10^{-16}$$

$$i_b := 4.30596 \cdot 10^{-23}$$

$$j_b := -2.7437 \cdot 10^{-20}$$

$$k_b := -6.782 \cdot 10^{-28}$$

$$B_{plexus}(z) := \frac{a_b + c_b \cdot z + e_b \cdot z^2 + g_b \cdot z^3 + i_b \cdot z^4 + k_b \cdot z^5}{1 + b_b + d_b \cdot z + f_b \cdot z^2 + h_b \cdot z^4 + j_b \cdot z^5}$$

$$i := 0..55$$

Calculating $B(z) + \Delta B(z)$

$$B_{1_{i+1}} := \left(B_{plexus}(i \cdot 1000) + \Delta B_1(i \cdot 1000) \right) \cdot \left(\text{cm}^{-1} \frac{\text{watt}}{\text{cm}^2} \right)$$

Converting new brightness temperatures into a temperature profile

$$T_{\text{spectrometer}_{i+1}} := \left| T(B_{1_{i+1}}) \right|$$

	1		
1	274.82		
2	274.21		
3	271.75		
4	268.97		
5	267.3		
6	267.53		
7	269.52		
8	272.57	K	
9	276.03		
10	279.51		
11	282.8		
12	285.86		
13	288.68		
14	291.26		
15	293.65		
16	295.87		

$T_{\text{spectrometer}} =$	$T_{\text{plexus}} := \begin{bmatrix} 290.233 \\ 286.949 \\ 281.901 \\ 275.579 \\ 268.449 \\ 260.924 \\ 253.355 \\ 246.023 \\ 239.15 \\ 232.909 \\ 227.433 \end{bmatrix} \cdot K$	$T_{\text{radiosonde}} := \begin{bmatrix} 274.8 \\ 266.2 \\ 262.2 \\ 261.0 \\ 257.7 \\ 252.6 \\ 245.9 \\ 240.0 \\ 233.7 \\ 226.3 \\ 218.1 \end{bmatrix} \cdot K$
-----------------------------	---	--

Calculated Temperatures
using spectrometer method

Plexus inputs

Actual Temperatures
from radiosonde

$$h := 1..10$$

Calculate difference between calculated temperature profile and radiosonde temperature profile.

$$\Delta T_h := T_{\text{spectrometer}_h} - T_{\text{radiosonde}_h}$$

	1	
1	0.019066430679402	
2	8.0123603635991	
3	9.55369440331771	
4	7.96902201582952	
5	9.60055267729683	K
6	14.9324461347775	
7	23.6155693849379	
8	32.5668106084541	
9	42.3318372053101	
10	53.207175648985	

Recover_Profile_3.MCD

ORIGIN \equiv 1

This mathcad template calculates a temperature profile assuming the change in the brightness temperature function is $\Delta B(z) := a_b + b_b \cdot z + c_b \cdot z^2$.

Assuming B is linear in form

$$\Delta B(z) := a_b + b_b \cdot z + c_b \cdot z^2.$$

Transmittance and kernel functions for 2567 cm $^{-1}$

$$a_{2567} := 0.99844082$$

$$b_{2567} := 0.00020672$$

$$c_{2567} := 0.00015199$$

$$d_{2567} := -2.112510^{10}$$

$$\tau_{2567}(z) := \frac{a_{2567} + c_{2567}z}{1 + b_{2567}z + d_{2567}z^2}$$

$$w_{2567}(z) := \frac{-(-c_{2567} + c_{2567}d_{2567}z^2 + a_{2567}b_{2567} + 2 \cdot a_{2567}d_{2567}z)}{(1 + b_{2567}z + d_{2567}z^2)^2}$$

Transmittance and kernel functions for 2568 cm $^{-1}$

$$a_{2568} := 0.99989574$$

$$b_{2568} := 0.00023758$$

$$c_{2568} := 0.0001878$$

$$d_{2568} := -1.657610^{10}$$

$$\tau_{2568}(z) := \frac{a_{2568} + c_{2568}z}{1 + b_{2568}z + d_{2568}z^2}$$

$$W_{2568}(z) := \frac{-(-c_{2568} + c_{2568}d_{2568}z^2 + a_{2568}b_{2568}z + 2 \cdot a_{2568}d_{2568}z)}{(1 + b_{2568}z + d_{2568}z^2)^2}$$

Transmissivity and Kernel functions for 2569 cm⁻¹

$$a_{2569} := 1.00035846$$

$$b_{2569} := 0.00024389$$

$$c_{2569} := 0.00019095$$

$$d_{2569} := -1.758910^{-10}$$

$$\tau_{2569}(z) := \frac{a_{2569} + c_{2569}z}{1 + b_{2569}z + d_{2569}z^2}$$

$$W_{2569}(z) := \frac{-(-c_{2569} + c_{2569}d_{2569}z^2 + a_{2569}b_{2569}z + 2 \cdot a_{2569}d_{2569}z)}{(1 + b_{2569}z + d_{2569}z^2)^2}$$

Solving for kernel functions coefficients

$$\int_0^{55000} \Delta B(z) \cdot W_{2567}(z) dz \text{ simplify } \Rightarrow 106132.1712504000000 \cdot c_b - .20070624872884911511 \cdot a_b - 828.13093544336896000 \cdot b_b$$

$$\int_0^{55000} \Delta B(z) \cdot W_{2568}(z) dz \text{ simplify } \Rightarrow -197940.92678280000000 \cdot b - .16454915550831362639 - 645.601385564716100000$$

$$\int_0^{55000} \Delta B(z) \cdot W_{2569}(z) dz \text{ simplify } \Rightarrow -18185.15202290000000 \cdot b - .17177825731653997457 - 662.134299768751000000$$

Weighting Function Coefficients

$$W := \begin{bmatrix} .20070624872884911511828.13093544336896000106132.1712504000000 \\ .16454915550831362639645.60138556471610000197940.9267828000000 \\ .17177825731653997457662.1342997687510000018185.15202290000000 \end{bmatrix}$$

Radiance values for 2567 cm-1, 2568 cm-1 and 2569 cm-1, respectively, from PLEXUS output.

$$L_{plexus} := \begin{bmatrix} 5.52430010^{-9} \\ 4.54500010^{-9} \\ 4.79820010^{-9} \end{bmatrix}$$

Radiance values for 2567 cm-1, 2568 cm-1 and 2569 cm-1, respectively, obtained using spectrometer.

$$L_{spect} := \begin{bmatrix} 1.38410^{-8} \\ 1.491 \cdot 10^{-8} \\ 1.19910^{-8} \end{bmatrix} \cdot \text{weight}$$

Calculate change in Radiance

$$\Delta L_1 := L_{spect} - L_{plexus}$$

Radiance difference for 2567 cm-1, 2568 cm-1 and 2569 cm-1, respectively.

$$\Delta L_1 = \begin{bmatrix} 9.3260210^{-9} \\ 1.14534310^{-8} \\ 8.0670710^{-9} \end{bmatrix}$$

Solving for the change in brightness temperature function, DB(z), coefficients

$$\text{coeff}_1 := W^{-1} \cdot \Delta L_1$$

$$\text{coeff}_1 = \begin{bmatrix} -1.896968963650760^{-7} \\ 3.766163063027040^{-11} \\ -2.30036652455620^{-14} \end{bmatrix}$$

$$a_{b1} := \text{coeff}_{1_1}$$

$$b_{b1} := \text{coeff}_{1_2}$$

$$c_{b1} := \text{coeff}_{1_3}$$

$$a_{b1} = -1.896968963650760^{-7}$$

$$b_{b1} = 3.766163063027040^{-11}$$

$$c_{b1} = -2.30036652455620^{-14}$$

$$\Delta B_1(z) := a_{b1} + b_{b1} \cdot z + c_{b1} \cdot z^2$$

Brightness temperature function used to calculate initial kernel functions

$$a_b := 3.9076510^{-7}$$

$$b_b := -2.0002 \cdot 10^{-4}$$

$$c_b := -1.1779 \cdot 10^{-10}$$

$$d_b := 5.95852 \cdot 10^{-8}$$

$$e_b := 1.586 \cdot 10^{-14}$$

$$f_b := -8.3255 \cdot 10^{-12}$$

$$g_b := -1.1398 \cdot 10^{-18}$$

$$h_b := 7.99827 \cdot 10^{-16}$$

$$i_b := 4.30596 \cdot 10^{-23}$$

$$j_b := -2.7437 \cdot 10^{-20}$$

$$k_b := -6.782 \cdot 10^{-28}$$

$$B_{plexus}(z) := \frac{a_b + c_b \cdot z + e_b \cdot z^2 + g_b \cdot z^3 + i_b \cdot z^4 + k_b \cdot z^5}{1 + b_b + d_b \cdot z + f_b \cdot z^2 + h_b \cdot z^4 + j_b \cdot z^5}$$

$$i := 0..55$$

Calculating $B(z) + \Delta B(z)$

$$B_{1,i+1} := (B_{plexus}(i \cdot 1000) + \Delta B_1(i \cdot 1000)) \cdot \left(\frac{\text{cm}^{-1} \cdot \text{watt}}{\text{cm}^2} \right)$$

Converting new brightness temperatures into a temperature profile

$$T_{\text{spectrometer}_{i+1}} := |T(B_{1,i+1})|$$

	1		
1	274.82	290.233	274.8
2	274.21	286.949	266.2
3	271.75	281.901	262.2
4	268.97	275.579	261.0
5	267.3	268.449	257.7
6	267.53	260.924	252.6
7	269.52	253.355	245.9
8	272.57	246.023	240.0
9	276.03	239.15	233.7
10	279.51	232.909	226.3
11	282.8	227.433	218.1
12	285.86		
13	288.68		
14	291.26		
15	293.65		
16	295.87		

$T_{\text{spectrometer}} = \begin{bmatrix} \cdot & \cdot & \cdot & \cdot \\ \cdot & \cdot & \cdot & \cdot \end{bmatrix} \text{K}$

$T_{\text{plexus}} := \begin{bmatrix} \cdot & \cdot & \cdot & \cdot \\ \cdot & \cdot & \cdot & \cdot \end{bmatrix} \text{K}$

$T_{\text{radiosonde}} := \begin{bmatrix} \cdot & \cdot & \cdot & \cdot \\ \cdot & \cdot & \cdot & \cdot \end{bmatrix} \text{K}$

Calculated Temperatures
using spectrometer method

Plexus inputs

Actual Temperatures
from radiosonde

$$h := 1..10$$

Calculate difference between calculated temperature profile and radiosonde temperature profile.

$$\Delta T_h := T_{\text{spectrometer}_h} - T_{\text{radiosonde}_h}$$

	1		
1	0.019066430679402		
2	8.0123603635991		
3	9.55369440331771		
4	7.96902201582952		
5	9.60055267729683		
6	14.9324461347775		
7	23.6155693849379		
8	32.5668106084541		
9	42.3318372053101		
10	53.207175648985		

$\Delta T = \begin{bmatrix} \cdot & \cdot & \cdot & \cdot \\ \cdot & \cdot & \cdot & \cdot \end{bmatrix} \text{K}$

APPENDIX 3: Radiosonde Data

This appendix contains radiosonde data for the two test cases. Radiosonde data is from the Wilmington OH radiosonde site, which is, located approximately 30 miles southeast from where the radiometric data was collected.

1 December 1999 0000Z RAOB

TTAA 51001 72426 99998 00058 01007 00309 // 92926 05956 35513 85581
12110 34513 70080 10965 35537 50561 24759 35059 40719 37563 35570 30910 54357
01086 25024 62556 36079 20163 57961 34076 15345 55173 34047 10604 57175 33029
88239 63156 35067 77307 01087 40805 51515 10164 00021 10194 // 35529=

UJXX 00KW 010000 72426
TTBB 51000 72426 00998 00058 11987 00960 22850 12110 33830 13510 44822 08564
55820 08375 66748 07988 77678 11362 88612 14563 99581 17964 11565 19960 22517
22962 33462 29756 44400 37563 55279 58556 66239 63156 77198 57162 88173 58967
99159 54972 11134 54176 22100 57175 31313 45202 82307 41414 856//=
99159 54972 11134 54176 22100 57175 31313 45202 82307 41414 856//=

8 December 1999 0000Z RAOB

USXX 00KW 080000 72426 TTAA 58001 72426 99986 02247 17005 00209 //
92838 02668 // 85527 07493 23023 70107 00689 23539 50571 18179 25038 40734
30723 25562 30932 45750 25583 25051 52562 26087 20193 57369 26575 15375 58373
26551 88189 58368 26077 77290 25093 42509 51515 10158 10164 00014 10194 //
24029=

UJXX 00KW 080000 72426 TTBB 58000 72426 00986 02247 11975 03458 22935
00656 33925 02668 44917 04674 55860 07296 66850 07493 77837 06873 88739 04286
99478 20977 11460 22966 22442 24736 33422 27316 44389 32321 55383 32157 66376
33160 77353 37156 88323 42358 99285 48737 11276 50547 22250 52562 33189 58368
44155 56775 55133 58974 66// 77123 61374 88120 61774 31313 45202 82302
41414 00900 51515 10150 10158=

Bibliography

BOMEM Inc. The MR Series Documentantation Set (1997).

Goody R. M., and Y. L. Yung. Atmospheric Radiation: Theoretical Basis (Second Edition). New York: Oxford University Press, 1989.

Hauser, R.G. Survey of Military Applications for Fourier Transform

Infrared (FTIR) Spectroscopy. MS Thesis, AFIT/GM/ENP/99M-07. School of Engineering Physics, Air Force Institute of Technology (AU), Wright-Patterson AFB OH,AFIT, Febuary 1999:

"PLEXUS." Release 3.0 Version 1.0. CD-ROM. Mission Research Corporation, May 1999

Schanda, E. Physical Fundamentals of Remote Sensing. Heidelberg : Springer-Verlag Berlin, 1986:

Smith, William L., H. E. Rvercomb, H. B Howell, H. M Woolf, R. O. Knuteson, R. G. Decker, M. J. Lynch, E. R. Westwater, R.G. Stauch, K. P. Moran, B. Stankov, M. J. Falls, J. Jordan, M. Jacobsen, W. F. Dabberdt, R. McBeth, G. Albright, C. Paneitz, G. Wright, P. T. May, and M. T.Decker. "GAPEX: A Groundbased Atmospheric ProfilingExperiment," Bulletin of the American Meteorological Society, 71: 310-318 (March 1990).

Theriault, J. M., "Retrieval of Tropospheric Profiles from IR Emission Spectra: Preliminary Results with the DBIS," SPIE, 2049: 119-128 (1993)

Theriault, J. M., C. Bradatte, and J. Gilbert, Atmospheric Remote Sensing with a Ground-based Spectrometer system. SPIE, 2744: 664-672 (1996)

Wallace, P. V. and Peter V. Hobbs. Atmospheric Science An Introductory Survey. New York: Academic Press, Inc., 1977

Vita

First Lieutenant Jon M. Saul was born on 7 May 1963 in Jacksonville, Florida. In August of 1981, he received his high school diploma from Florida Junior College at Jacksonville. In June of 1989, he completed degree requirements and was awarded an associate degree in Electrical Engineering from the Community College of the Air Force. In 1993, he was selected for the Airman's Education and Commissioning program to complete a baccalaureate's degree in meteorology from Florida State University and graduated in April of 1996. In August of 1996, he completed Officer Training School at Maxwell AFB, Mississippi. In August of 1998, he entered the Air Force Institute of Technology at Wright-Patterson AFB, Ohio, to complete requirements for a master's degree in meteorology.

Lieutenant Saul entered the United States Air Force in May of 1985, where he completed basic training. Following basic training, he received technical training at Keesler AFB, Mississippi, as a Ground Radio Technician. His first assignment was to Torrejon AB, Spain, in 1986, where he served as a Ground Radio Technician. In May of 1988, he was transferred to Kelly AFB, Texas, where he performed duties as an equipment installer, followed by a shop foreman, and finally as an engineering technician for the Air Intelligence Agency. After completing Officer Training School, he was reassigned to Kadena AB, Japan, where he served as a Wing Weather Officer. Upon graduation from the Air Force Institute of Technology, he will be assigned to the Starfire Optical Range at Kirkland AFB, New Mexico.

REPORT DOCUMENTATION PAGE

Form Approved
OMB No. 0704-0188

Public reporting burden for this collection of information is estimated to average 1 hour per response, including the time for reviewing instructions, searching existing data sources, gathering and maintaining the data needed, and completing and reviewing the collection of information. Send comments regarding this burden estimate or any other aspect of this collection of information, including suggestions for reducing this burden, to Washington Headquarters Services, Directorate for Information Operations and Reports, 1215 Jefferson Davis Highway, Suite 1204, Arlington, VA 22202-4302, and to the Office of Management and Budget, Paperwork Reduction Project (0704-0188), Washington, DC 20503.

1. AGENCY USE ONLY (Leave blank)	2. REPORT DATE	3. REPORT TYPE AND DATES COVERED	
	March 2000	Master's Thesis	
4. TITLE AND SUBTITLE Atmospheric Temperature Profiles By Ground-based Infrared Spectrometer Measurements			5. FUNDING NUMBERS
6. AUTHOR(S) Jon M. Saul, First Lieutenant, USAF			
7. PERFORMING ORGANIZATION NAME(S) AND ADDRESS(ES) Air Force Institute of Technology Graduate School of Engineering and Management (AFIT/EN) 2950 P Street, Building 640 WPAFB OH 45433-7765			8. PERFORMING ORGANIZATION REPORT NUMBER AFIT/GM/ENP/00M-11
9. SPONSORING/MONITORING AGENCY NAME(S) AND ADDRESS(ES) AFRL/VSBM ATTN: Capt Roy Calfas Hanscom AFB, MA 01731			10. SPONSORING/MONITORING AGENCY REPORT NUMBER DSN 487-3645
11. SUPPLEMENTARY NOTES Chairman: Lt Col Glenn P. Perram, ENP, DSN: 785-3636, ext. 4511 Member: Dr Mark E. Oxley ENP, DSN: 785-3636, ext. 4645 Member: Major Devin J. Della-Rose, ENP, DSN: 785-3636, ext.			
12a. DISTRIBUTION AVAILABILITY STATEMENT APPROVED FOR PUBLIC RELEASE; DISTRIBUTION UNLIMITED.		12b. DISTRIBUTION CODE	
13. ABSTRACT (Maximum 200 words) A method to recover atmospheric temperature profiles using a ground-based Fourier Transform Infrared spectrometer was investigated. The method used a difference form of the radiative transfer equation, a Bomem MR series Fourier Transform Infrared Spectrometer to collect atmospheric radiance values, and the Phillips Laboratory Expert-assisted User Software (PLEXUS) atmospheric radiance model, to recover an atmospheric temperature profile. The method researched uses radiance values from both the spectrometer measurements and the atmospheric model, along with kernel functions calculated by the atmospheric model as input to a difference form of the radiation transfer equation. From this the change in brightness temperatures was determined. The method assumes that the actual brightness temperature profile is a summation of a standard or reference brightness temperature profile plus some change in the brightness temperature. The brightness temperature profile used by the atmospheric model is the reference brightness temperature profile. Planck's Law was employed to transform the calculated brightness temperature function into a temperature function. A temperature profile was retrieved, although significant differences existed between the recovered temperature profile and a radiosonde recovered temperature profile.			
14. SUBJECT TERMS Ground-based Remote Sensing, Spectrometer, Temperature Profiling, Infrared			15. NUMBER OF PAGES 69
16. PRICE CODE			
17. SECURITY CLASSIFICATION OF REPORT UNCLASSIFIED	18. SECURITY CLASSIFICATION OF THIS PAGE UNCLASSIFIED	19. SECURITY CLASSIFICATION OF ABSTRACT UNCLASSIFIED	20. LIMITATION OF ABSTRACT UL